Integration of Structural Health Monitoring and Asset Management

Prepared by

Virginia Tech Transportation Institute

The Pennsylvania State University ❖ University of Maryland
University of Virginia ❖ Virginia Polytechnic Institute and State University ❖ West Virginia University

INTEGRATION OF STRUCTURAL HEALTH MONITORING AND ASSET MANAGEMENT

Linbing Wang, Ph.D., P.E., Professor

Wenjing Xue, Ph.D. Candiate

Cris Druta, Ph.D., Senior Research Associate

Dong Wang, Ph.D.， Research Associate

Center for Smart Infrastructure and Sensing Technology

Virginia Tech Transportation Institute

December 2012

1. Report No. MAUTC-2009-01 VT	2. Government Accession No.	3. Recipient's Catalog No.
4. Title and Subtitle Integration of Structural Health Monitoring with Asset Management		5. Report Date December 2012
		6. Performing Organization Code
7. Author(s) Linbing Wang, Wenjing Xue, Cris Druta, Dong Wang		8. Performing Organization Report No. MAUTC-2009-01 VT
9. Performing Organization Name and Address Virginia Tech Virginia Tech Transportation Institute Blacksburg, VA		10. Work Unit No. (TRAIS)
		11. Contract or Grant No. DTRT07-G-0003
12. Sponsoring Agency Name and Address Virginia Department of Transportation 1401 E. Broad St. Richmond, VA 23219 U.S. Department of Transportation Research and Innovative Technology Administration UTC Program, RDT-30 1200 New Jersey Ave., SE Washington, DC 20590		13. Type of Report and Period Covered Final Report June 2009 – June 2012
		14. Sponsoring Agency Code

15. Supplementary Notes

16. Abstract
The Virginia Center for Innovation and Transportation Research and Virginia Tech installed a structural health monitoring (SHM) system on a Virginia bridge. Using data from this SHM system as input, a procedure was developed to provide information on the lane occupancy, speed, classification and gross vehicle weight of heavy trucks. The resulting information is very useful for bridge management. The data also augments existing bridge WIM data collection sites in Virginia. The procedure could add functionality to other bridge SHM systems in Virginia. The system provides useful information on truck loading at low cost.

17. Key Words	18. Distribution Statement
Structural health Monitoring, Asset Management, Bridge Management, Bridge Weight-in-Motion	No restrictions. This document is available from the National Technical Information Service, Springfield, VA 22161

19. Security Classif. (of this report)	20. Security Classif. (of this page)	21. No. of Pages	22. Price
Unclassified	Unclassified		

Table of Contents

Table of Figures

Table of Tables

LITERATURE REVIEW

Pavement is important for economy and society as being an essential part of the transportation system. In the last decades, Pavement Management System (PMS) has brought many benefits to the socialized transportation system. The concept of "Smart Road" is being implemented with a variety of advanced technologies devoted to different intelligent responses, and one essential component of Smart Road is pavement monitoring. The strategies and decisions from PMS are based on various observations and measurements of the pavement or Pavement Monitoring. As an essential component of PMS, pavement assessment (low frequency monitoring, referred as pavement monitoring as well hereafter) and pavement monitoring have attracted much more attention and been improved via various advanced technologies and methodologies in recent years.

Surface Condition and Pavement Deflection Assessment

The surface conditions of pavements, including the occurrence and severity of cracking, rutting, wear, deflection and other distresses present on pavement surface, are an important indicator of pavement performance. The Long-Term Pavement Performance (LTPP) program has collected pavement surface conditions and many other pavement performance measures on a variety of pavements, and most state transportation agencies have collected pavement distress data for pavement management in recent years[1].

Surface cracking is an obvious and important distress indicator of pavement performance. Conventional visual and manual pavement cracking analysis approaches can be used to monitor the surface conditions. However these traditional methods are very costly, time-consuming, unsafe to inspectors, labor-intensive, and subjective[2]. All the drawbacks led people to explore more advanced, safer and more efficient methods for pavement surface condition assessments. Since 1990s, evaluation of pavements using digital imagery has become increasingly popular as a result of the significant leap in the sciences of computer vision and image processing[3]. In 1991, Mohajeri and Manning developed an approach to process segmented pavement distress images with directional filters[4]. In 1993, Koutsopoulos and Downey explored statistical algorithms for image enhancement, segmentation and distress classification[5]. Many

sophisticated techniques have been studied to improve the accuracy of classification[6, 7], and among which the theory of Fuzzy sets is the most popular one[2, 8].

Surface deflection is a reliable pavement structural response indicator[9], and has been measured in many pavement monitoring projects. In 1971, the NAPTF (National Airport Pavement Test Facility) failure criterion was established through the US Army Corps of Engineers' (US COE) Multi-Wheel Heavy Gear Load (MWHGL) test conducted at Vicksburg, Mississippi[10]. In 2000, the deformation of a pavement within the Newcastle University Rolling Load Facility (NUROLF) was measured by stereo-imagery using both analytical and digital photogrammetry[11]. In 2001, McQueen et al.[12] validated the linear load-deflection relationship of the NAPTF HWD test results. Gopalakrishnan[13] introduced a Heavy Weight Deflectometer (HWD) test to monitor the effect of simulated Boeing 777 and Boeing 747 aircrafts on pavement condition.

The schedule for pavement monitoring, called monitoring frequency, has some impact on pavement performance prediction, and pavement decision making in the end [14]. To assess the conditions of pavements, most highway agencies collect the condition data annually, biannually and triannually [15]. According to the study of Haider et. al in 2011[14], "monitoring interval may affect the short- and long-term network conditions for various preservation strategies", "monitoring cracking (image based) at a 1-year interval will be more appropriate, whereas for roughness (sensor based); a monitoring interval of 1 to 2 years could be suitable".

In-Situ Pavement Health Monitoring Sensors

As described in the previous sections, the monitoring of pavement condition can be conducted by visual investigation and various other testing methods. Most of these methods can be used on any pavement of interest, having the advantages of spatial flexibility. In contrast, monitoring systems with sensing devices installed in pavement has also been extensively investigated to achieve real-time monitoring, which has frequency superiority of pavement monitoring

Pavement health monitoring is essential in pavement management and critical to the socialized and integrated transportation system. The accurate measurement of the strain and stress

distributions in pavement is critical for the understanding of pavement behavior and the modeling of pavement failure. Tremendous efforts have been devoted to in situ monitoring by governments and transportation agencies around the world. After several decades' research and application, a wide variety of sensors has been developed for in-situ pavement monitoring, and most of the sensors can be classified into two categories: electromagnetic sensor and optical fiber sensor.

The application of electromagnetic sensors in pavement monitoring can be traced back to the 1960s[16]. In 1991, Sebaaly et al.[17] tested various types of pavement instrumentation, including pressure cell, deflectometer, strain gauge, thermocouple, moisture sensor, and transverse vehicle location sensor, for field evaluation under actual truck loading. In 1995, Sebaaly et al.[18] measured the tensile strains in flexible pavement using the Hall Effect sensor in an H-gage configuration. In 2001, commercial diaphragm-type stress cells were embedded in subgrade to compare the performance of two instrumented pavement test sections under linear traffic simulator[19]. In 2005, Huff et al.[20] investigated piezoelectric axle sensors to obtain dynamic pavement deflection data. In 2011, Xue and Weaver [21] explored the effect of wide-base tire on pavement strain response based on the data collected from SPS-8 on Ohio-SHRP U.S. 23 Test Road in 1997. In the same year, a novel self-powered wireless sensor was developed based on the integration of piezoelectric transduction with floating-gate injection, which is also capable of detecting strain and temperature simultaneously [22].

Fiber optics sensors have attracted lots of efforts in civil engineering infrastructure monitoring because of several of its positive attributes, including distributed sensing capabilities, small diameter, light weight, immunity to electromagnetic interference, strong survival ability and high sensitivity[23, 24]. In 1994, Navarrete and Bernabeu[25] described an interferometry system, which can detect changes in pressure on fiber and measure another external stimulus and changes simultaneously. In 1995, Signore and Roesler [26] used fiber-optic sensors to study the lateral strain behavior of axially loaded emulsified asphalt specimen and obtained its Poisson ratio. In 1996, polymide multimode fiber was braided for increased sensitivity. In 2005, Wang and Tang[27] developed a new high-resolution fiber Bragg grating (FBG) sensor consisting of a referenced FBG and a pair of fiber gratings, and provided the potential of simultaneous

measurement of strain and temperature within pavements. Due to the increasing interest of the response and performance in the whole structure, 3-dimensional monitoring has gained more and more attention. In 2012, Zhou et al. set up a 3D optical fiber grating based sensor assembly [28].

Integrated Monitoring System

With the development of information technology and digitization, traditional pavement monitoring systems have been integrated with other monitoring systems, including bridge monitoring, Weigh-in-Motion (WIM), traffic classification and so on. Both electromagnetic and optical fiber optic sensors have been widely studied and used in various integrated pavement monitoring systems.

For better understanding of pavements, various pavement research facilities (test roads) have become an integral of pavement research and engineering, and the foremost was the AASHO Road Test conducted in Ottawa, Illinois from 1958 to 1960[29].As early as in 1989, Rollings and Pittman presented the result of instrumental model tests and full-scale traffic test on rigid pavement, which matched the Westergaard edge-loaded analytical model well on design stresses[30]. In 2004, eight sections were fully instrumented to measure in situ pavement responses under load at the NCAT test track[29]. Timm et al.[31] presented the data collection and processing procedures for the NCAT test track instrumentation. MnROAD in Minnesota was heavily instrumented with 40 test cells; based on the monitored data Lukanen developed mechanistically based load equivalency factors (LEF) in 2005[32]. The Virginia Smart Road is another outdoor pavement research facility located in Blacksburg of Virginia, which has twelve instrumented sections [33]. In 2006, Loulizi et al. [34] used one section of the Virginia Smart Road to compare measured stress and strain, and obtained the difference between the stresses and strains measured in situ and calculated for a flexible pavement section.

Many bridges worldwide are closely monitored because of their economic importance and vulnerability to extreme loading and harsh environmental conditions[35]. The monitoring of bridges is convenient to be integrated with pavement monitoring because of their similarity in structure and function. The monitoring system of Geumdang Bridge in Korea using high-resolution wireless sensors are combined together with the two-lane passing test road which

employed 1897 sensors to evaluate three types of pavement constructed along the road length[36]. In Hong Kong, the integrated monitoring system with more than 800 sensors permanently installed on the three long-span cable-supported bridges- the suspension Tsing Ma Bridge, the cable-stayed Kap Shui Mun Bridge, and the Ting Kau Bridge[37]. In United States, the Commodore Barry Bridge is instrumented using 77 sensors and 115 channels to track the loading environment and structural responses, and expected to be integrated with a WIM system in the future[38]. In 2012, Kim and Lynch[39] installed wireless sensors on both the bridge and moving vehicle and record the dynamic interaction between the bridge and vehicle.

Weigh-in-Motion (WIM) system is used to obtain the weight of a vehicle while the vehicle travels at low speed. Since the concept was brought up sixty years ago[40], WIM technologies have been used increasingly around the world for weight control of heavy vehicles, the protection and management of pavement and other infrastructures[41]. For example, there are more than 100 Weigh-in-Motion stations throughout California by 2002 [42]. Today there are several major types of sensors used for WIM stations: piezoelectric sensors, capacitive mats, bending plate, load cell and optic fiber[41, 43]. The original highway WIM system[44] used weighing devices in one lane of the road. As early as 1989[45], a high speed Weigh-in-Motion system which was manufactured and supplied by International Road Dynamics (IRD), was installed on Highway 1 near Regina of Canada.

During the past twenty years, each kind of WIM station has been widely studied and developed by worldwide scholars and transportation agencies. Due to the distributed sensing properties, high environment resistance, and other advantages, the studies and applications of optic fiber sensors in WIM systems increased significantly in the past 10 years [23, 46-49]. In 2007, Cheng et al.[50] presented the design of a new capacitive flexible weighing sensor for a vehicle WIM system. In the same year, Zhang et al[51] investigated a novel WIM system based on multiple low cost, light weight, small volume and high accuracy embedded concrete strain sensors.

Vehicle classification is another important category of traffic data collection. The study of vehicle classification can be traced back to 1976[52], and commercial detector equipment was used to measure some configuration parameters of a passing vehicle with rough estimation. As of

today, lots of information and sensing technology have been devoted to improving the classification. Vehicle classification technologies in current use can be grouped into three major categories: axle based, vehicle length based, and machine vision (visual) based[53]. In recent years, the most popular sensing technologies used in vehicle detecting are piezoelectric sensor, inductive loops, and fiber optic sensors. Piezoelectric sensor is the most widely instrumented, and a lot of experience has been accumulated. In 1990s, cheaper inductive loops (usually single loop or dual loop detectors) were developed to replace the expensive piezoelectric sensors with high classification efficiency preserved [54-58]. Fiber grating sensor application in traffic classification increases because of its advantages and its wide application in pavement health monitoring and Weigh-in-Motion system. Efforts of scholars throughout the world are devoted to improving its performance in vehicle classification [59-62]. At the same time, some other researchers devoted efforts to making use of traditional sensors for health monitoring to detect and classify vehicles. In 2008, Zhang et al.[63] delivered a new vehicle classification method and developed a traffic monitoring detector with embedded concrete strain gauges.

WIM systems and vehicle classification system mentioned above, together with vehicle speed measurement, are all parts of traffic data collection. "Truck data collection and reporting is an important program that state departments of transportation (DOTs) must maintain to comply with FHWA requirements"[53]. For example, the Florida Department of Transportation (FDOT) has approximately 350 traffic classification and WIM sites located throughout the state, including thousands of piezoelectric sensors [64]. Due to the low survival rate of piezoelectric sensors, FDOT was committed to the development of optical fiber sensors in traffic classification and WIM system because of its flexibility, corrosion resistance and immunity to electromagnetic interference[65]; in this project, Cosentino and Grossma developed a fiber optic traffic sensor (FOTS) in 1996[66]; they improved its sensitivity, validated its application in both flexible and rigid pavements, and explored its WIM accuracy in 1997[67]; finally they deployed the designed fiber optic traffic sensor in monitoring system for traffic classification and WIM system in 2000[68]. Since June 2008, an in situ measuring station has been used in Lenzburg, Switzerland[69]. This measuring station includes Weigh-in-Motion sensors, Stress-in-Motion sensors, temperature sensors and acceleration sensors, and serves as a useful tool for both the statistical assessment of traffic and the loading condition of the pavement.

Summarized Development of Monitoring Systems in Pavements

Pavement monitoring is very important to transportation management, and has been a hotspot of transportation research since the middle of 20th century. The broad concept of pavement monitoring includes pavement assessment (monitoring with low frequency) and in-situ pavement monitoring.

For pavement assessments, the surface conditions of pavement (cracking and deflection) are measured to evaluate its performance. Lots of sensing and measuring technologies have been developed to replace the traditional visual and manual methods.

In-situ pavement monitoring means obtaining the pavement responses via the sensing devices fixed in/around pavement, and realizes the timing flexibility of data collection. The sensing devices installed in pavement can be categorized into electromagnetic and fiber optic sensors according to their signal transferred, and both of them have been studied a lot on sensitivity, functionality, scale, living rate and resistance to harsh environment. As a result, pavement monitoring system has been improved on accuracy, scale, lasting, comprehensiveness, and other factors.

Other related monitoring systems, such as bridge monitoring, Weigh-in-Motion (WIM), traffic classification systems, are also described and reviewed. They can be integrated with pavement monitoring effortlessly because of their similar structure and function, and tremendous potential benefit can be expected.

As a summary of the review, the described developments of in situ pavement monitoring systems, and other monitoring systems which can be integrated with pavement monitoring system are listed in TABLE 1.

TABLE 1 Summary of Recent Development in Monitoring Systems in/for Pavement

Purpose of Monitoring System	Year	Authors/Infrastructure	Measurement	Sensing Type	Sensors	Note
Pavement Health Status	1946[30]	Rollings and Pittman	Strain	EM	Strain gage	Full-scale, accelerated

						traffic tests
	1991[17]	Sebaaly et al.	Stress; deflection; strain; temperature; moisture; vehicle location.	EM	NA	NA
	1994[32]	MnRoad, Minnesota	Stress, strain, applied loading	EM	WIM devices, temperature, moisture, thermal strain sensors	Both rigid and flexible pavements
	1995[18]	Sebaaly et al	Strain	EM	Strain gage	Hall-effect gage
	1995[26]	Signore and Roesler	Strain	FO	NA	Laboratory test
	1997[21]	US 23 Test Road, Ohio	Strain	EM	Strain gage	NA
	1998[33, 34]	The Virginia Smart Road, Virginia	Stress, strain, temperature, moisture, frost penetration	EM	Pressure cell, strain gauges, thermocouple, reflectometry and resistivity probes.	NA
	2001[19]	Goncalves et al.	Stress	EM	Diaphragm-type stress cell	Full-scale, accelerated traffic tests
	2004[29, 31]	NCAT	Strain, stress, moisture and temperature	EM	Strain gage, pressure cell, moisture probes and thermistor	NA
	2005[20]	Huff et al.	Digitized current	EM	Piezoelectric axle sensor	NA
	2005[27]	Wang and Tang	Strain and temperature	FO	Fiber Bragg Grating Sensor	Measure strain and temperature simultaneously
	2011[22]	Lajnef et al.	Strain and temperature	EM	Piezoelectric transduction	Self-powered piezo-floating-gate array
	2012[28]	Tailai Highway, China	Strain	FO	OFBG	3D monitoring
Bridge Monitoring	2000[70]	Tsing Ma Bridge, Kap Shui Mun Bridge and Ting Kau Bridge, Hong Kong	Strain/stress, displacement, acceleration, temperature, wind, axle load	EM	NA	Wind and Structural Health Monitoring System (WASHMS)
	2000[38]	Commodore Barry Bridge, New Jersey	Wind, strain and acceleration.	EM	Strain gages, piezoelectric accelerometers and ultrasonic anemometer	NA

	2006 [71, 72]	Alamosa Canyon Bridge, New Mexico	Acceleration	EM	NA	NA
	2006[36]	Geumdang Bridge, Korea	Acceleration	EM	piezoelectric and capacitive	Traditional tethered and wireless
	2012[39]	Yeondae Bridge, Korea	Acceleration and tactility	EM	capacitive accelerometer and piezoelectric tactile sensor	Vehicle-bridge interaction
WIM	1986[45]	Highway 1, Canada	Load, speed	EM	IRD-WIM-5000 system and radar	NA
	1994[25]	Navarret and Bernabeu	Pressure	FO	NA	Mach-Zehnder interferometer
	2004[46]	Yuan et al.	Pressure	FO	NA	Michelson interferometer
	2007[43]	Cheng et al.	Strain	EM	Capacitive sensor	Light weight, small volume and portability.
	2008[23]	Malla et al.	Load	FO	NA	Two concentric light guiding regions
Vehicle Classification	2001[54]	Gajda et al.	Inductive voltage	EM	Inductive loop detector	Cheap
	2002[60-62]	Interstate 84 in Oregon	Amplitude of optical signal	FO	NA	NA
	2003[57]	Interstate 710 in California	Traffic volume, vehicle length and speed	Em	Single inductive loop detector	NA
	2009[55]	I-70 and I-71, OHIO	Inductive voltage	EM	Single-loop, Dual-loop and Piezoelectric detector	NA
Integrated Traffic Data Collection	2000[65-68]	Cosentino and Grossman	WIM; vehicle classification	FO	Fiber optic traffic sensor (FOTS)	Microbend fiber-optic sensing technology
	1988[64]	Florida	WIM and vehicle classification	EM	Piezoelectric sensor, loop detector, and bending plate	More than 300 continuous monitoring sites
	2008[69]	A1 motorway, Switzerland	Vehicle weight, traffic classification, temperature, acceleration	EM	WIM, Stress-in-Motion, temperature and acceleration sensors	Footprint measuring station
	2008[51, 63]	Zhang et al.	WIM and vehicle classification	EM	strip strain sensor	Simple and efficient

NA = not available

INTRODUCTION

Proposed Research

Currently, an integrated transportation monitoring system was developed at Virginia Tech Transportation Institute, which was funded by the collaborative project "Integrated Infrastructure Asset Monitoring Assessment and Management". This project investigated the feasibility and potential benefits of the integration of infrastructure monitoring systems into transportation management system.

This wireless monitoring system is located on Route 114 in Christiansburg, Virginia. The instrumentation was devised to provide asphalt pavement responses of strain, stress, temperature and moisture . The gauges selected included CTL horizontal and vertical strain gages, load cells, thermocouples and a moisture probe. The installation was conducted as part of an VDOToverlay project. Wireless voltagenodes, connected to analog sensors, were positioned by the side of the road to receive/send the signal to the computer .

experiments were conducted to develop a back calculation methodology. The purpose of this transportation monitoring system is to monitor both traffic and pavement conditions. When finished, it will serve as a Weigh-in-Motion system and traffic classification system in addition to collecting the mechanical response and monitoring the health status of the pavement. A novel back calculation method based on a distribution model will be present for estimating a vehicle's speed, wandering, number of axles, distance between axles, distance between wheels, and axle weights.

Experimental Methods

analog SensorsThe designed wireless monitoring system has two components: analog sensors and wireless voltage nodes. There are four kinds of analog sensors involved in the experiment, including strain gauges, load cells, thermocouple and moisture probes. technical data is provided in Appendix A.

Horizontal and vertical strain gages used in the experiment are from CTL Company. CTL Asphalt Strain Gauge is a field proven design to ensure accurate long-term data collection. It uses durable materials to withstand the high temperature and compaction loads in pavement construction. The parameters and figures of the strain gages are listed as the following:

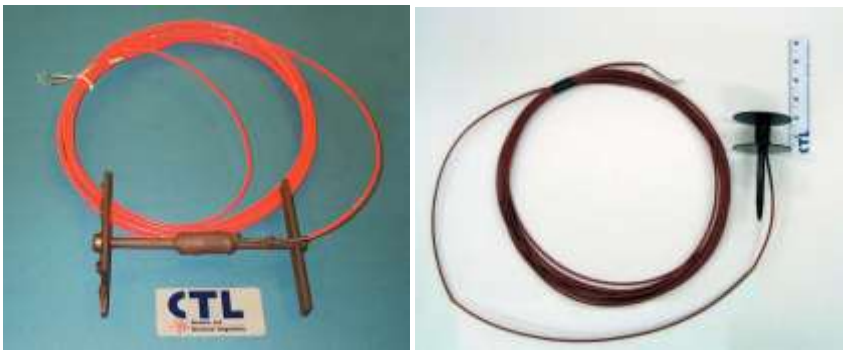

Figure 1: CTL Horizontal and Vertical Strain Gauges

The calibration of all the strain gauges used in this study was performed using the strain wizard feature, supplied by the "MicroStrain software". The necessary parameters for strain wizard are listed in Table 2.

Table 2: Parameters in Software "MicroStrain Node Commander 2.4.0"

Bridge Type	Full Bridge
Number of Active Gauges	4
Gauge Factor	2.00
Gauge Resistance	350 ohm
Shunt Resistance	499000 ohm

The KDE-PA Soil Pressure Gauge (Figure 2) from Tokyo Sokki Kenkyujo Company was used in the experiment as load cell.

Figure 2: KDE-PA Soil Pressure Gauge

The load cell can be calibrated as in Eq. (1). Same calculations apply to all the load cells and the results are summarized in Table 3.

$$\text{Calibrated Slope} = \frac{\text{Sensor Capacity}}{\text{Rated Output} \times \text{Excitation Voltage} \times \text{Gain} \times \text{Transition Rate}}$$
$$= \frac{145 \text{ psi}}{484 \ \frac{\mu v}{v} \times 3 \ v \times 210 \times \frac{4096 \ bits}{3 \text{ v}}} = 0.348292 \text{ psi/bit} \qquad \text{Eq.(1)}$$

Table 3: Calculation results for all the load cells

Sensor	Serial No.	Rated Output	Calibrated Slope
A1	KDE-1MPA-EBJ100014	484	0.348292
A2	KDE-1MPA-EBJ110034	620	0.271892
B1	KDE-1MPA-EBJ110035	575	0.293171
B2	KDE-1MPA-EBJ110036	584	0.288621

The thermocouple TMTSS-125-6 from Omega Company was used to measure the pavement temperature in the experiment.

Figure 3: Thermocouple TMTSS-125-6

The thermocouple was calibrated using a mercury-filled thermometer in water. Testing results are summarized in Figure 4, and the linear trend line was used for future temperature calibration input data.

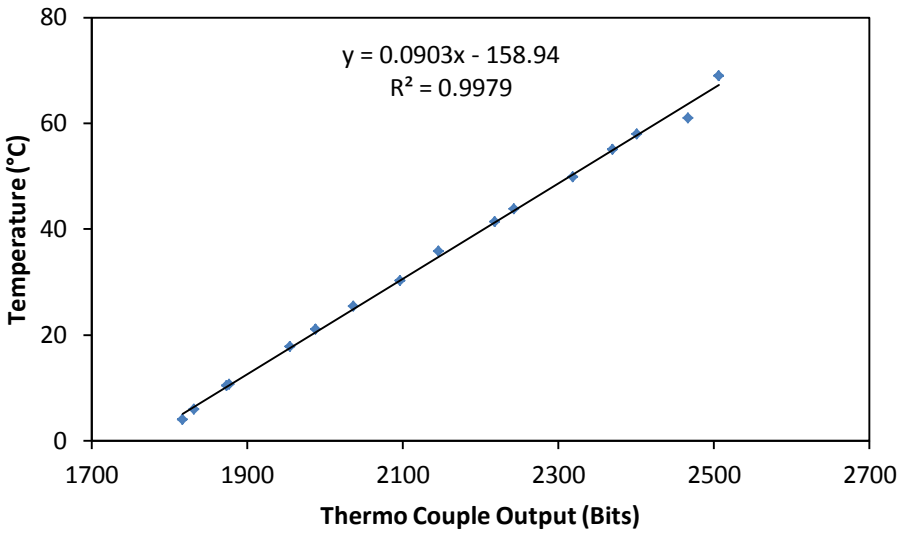

Figure 4: Calibration of Thermo Couple TMTSS-125-6

VH400 Soil Moisture Sensor Probe, used in the experiment to measure moisture was from Vegetronix Company. It measures the dielectric constant of the soil using transmission line techniques. It is insensitive to water salinity, and does not corrode over time like the conductivity based probes.

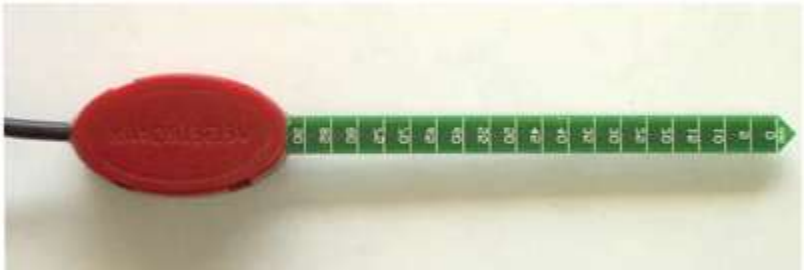

Figure 5: VH400 Analog Soil Moisture Sensor Probe

The moisture sensor was calibrated by increasing the moisture content in soil samples of known weight. The relationship between the output reading (bits) and the moisture content (%) is plotted in Figure 6.

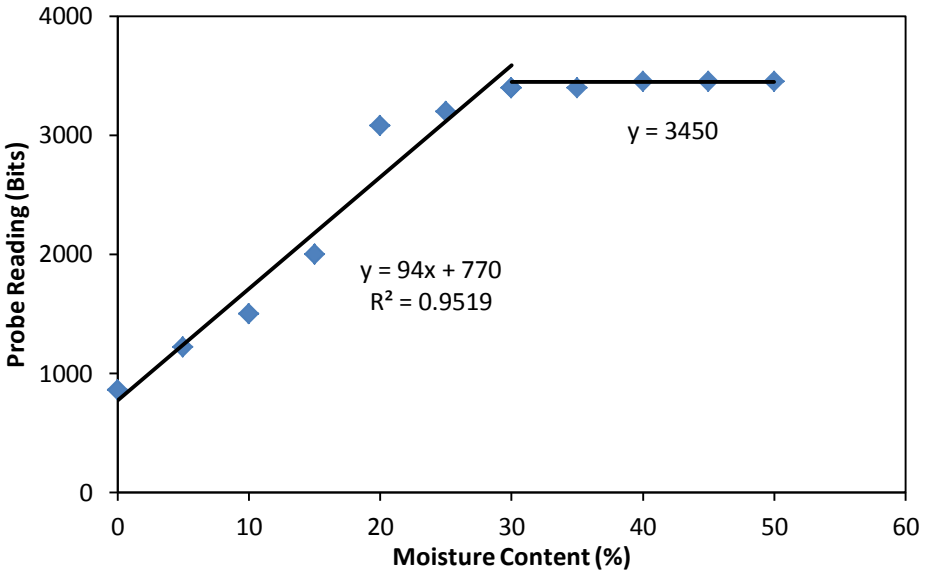

Figure 6: Calibration Data for the VH400 Soil Moisture Probe

The V-Link wireless voltage nodes were part of a high speed wireless sensor network. In the monitoring process, data is transferred wirelessly from the node to the base station connected to the computer. The maximum voltage the V-Link node can supply to the sensors for readings is 3 V. The V-Link nodes and the USB base station used in the project are shown in Figure 7, and the specifications are listed in Appendix B

Figure 7: V-Link Wireless Voltage Node and USB Base Station

Instrumentation

The experimental section is located on Virginia Route 114. Some archived plans show that this pavement section of predates the 1940's, and has been manipulated several times with the opening of the Radford Arsenal, the opening of the second New River bridge and various

maintenance activities that might have taken place over the past 70 – 100 years. It is nearly impossible to tell the existing pavement structure accurately without coring the pavement. According to the nearest cores (approximately 1 mile away) that VDOT provided, the thickness of the top layer is set to be 3 inch, and the baselayer is 7 inch thick.

The pavement installation of the sensors was conducted during overlay operations as part of VDOT rehabilitation program for 2011. The sequence of operations were:

a. Marking the locations and shapes of the sensors on the pavement as in **Error! Reference source not found.**(a);
b. Cut following markings and remove the asphalt concrete in **Error! Reference source not found.**(b)??;
c. Place sensors in cut holes Set the cables in the trench following the layout;
d. Cover the embedded sensors and cables with hot mixed asphalt concrete .
e. The paver passes by, compact the asphalt concrete and leaves a 1.5 inch thick overlay, as shown in **Error! Reference source not found.**(c);
f. Neaten and storage the output cables in a box by the side of the pavement, as in **Error! Reference source not found.**(d).

Figure 8: Installation Procedure (a. marking, b. cutting, c. paver passing, d. output cable management)

Due to the funding limits, sensor distribution is designed to cover all necessary points of the back calculation with fewest sensors. Several groups of sensors are arranged on the important position of the transverse plane. Each group includes load cell, vertical strain gauge, horizontal strain gauge in longitudinal plane, and horizontal strain gauge in transverse plane, with 1 foot apart from each other. Five horizontal strain gauges are arranged in a straight line to make sure of the vehicle passing position in the transverse plane. The final layout is shown in Figure 9.

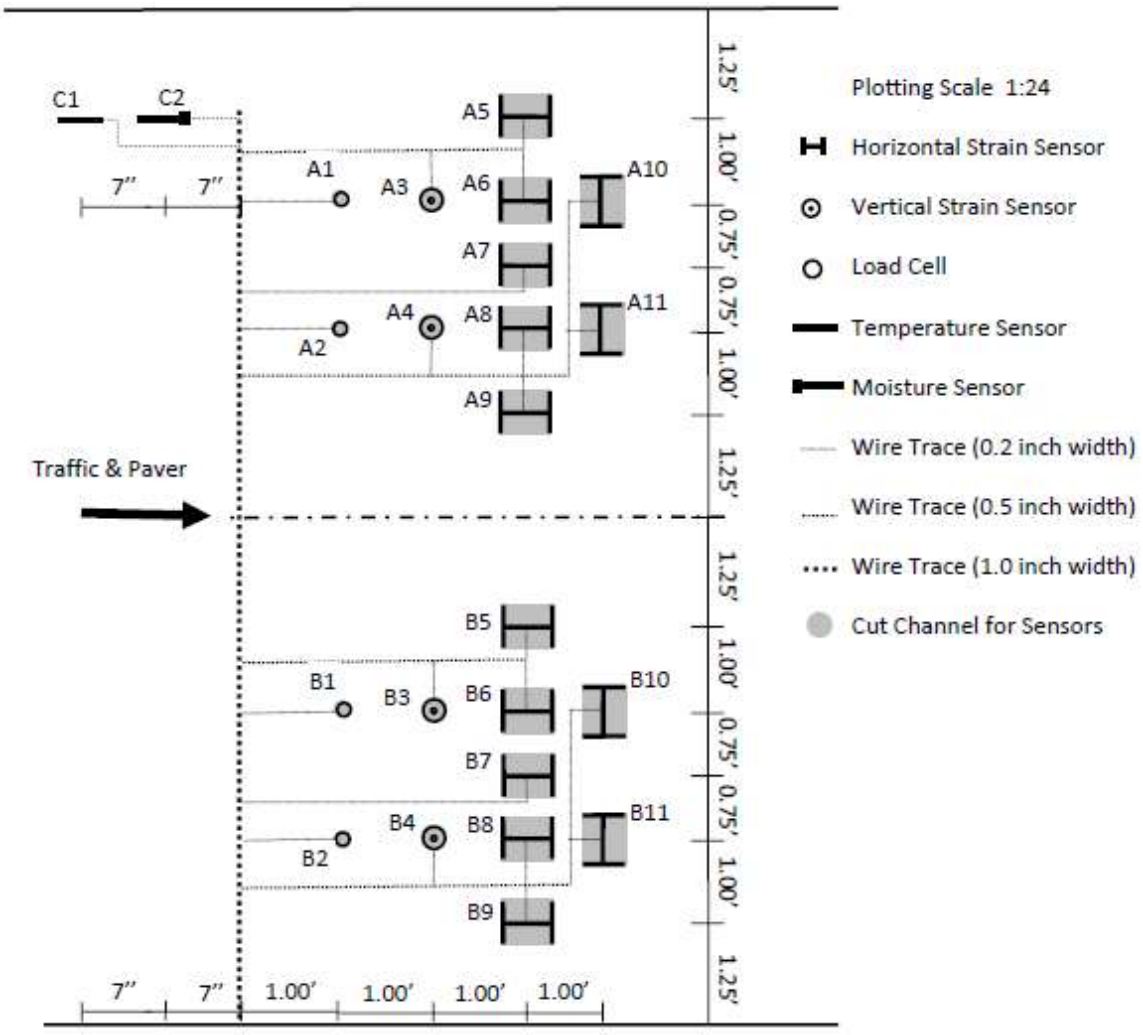

Figure 9: Sensor Distribution and Layout

Data Collection

The data logging is performed as follows:

- Connect the wireless nodes and the output gauges cables
- Run the "Node Command", software on the laptop with base station plugged in;
- setup all the wireless nodes in the network;
- Calibrate and configure for each wireless node;
- Start the data logging

During tests, the test vehicle passes the experimental section at constant speed, and all the pavement responses are recorded for the back calculations. The obtained strain, stress, temperature and moisture data are stored in the laptop and ready to be used for the further analysis. The data logging obtained by wireless node is stored with the sweep numbers, and the sweep rate is necessary to the calculation of time interval and specific time points. The sweep rate for different wireless nodes is different for continuous streaming mode.

for data acquisition, a van was used in the experiment to provide a known loading condition. According to the truck scale in Virginia Tech Transportation Institute, the weight of the van is 6340 lb (±20 lb) with half tank of gas and back two benches removed. Considering the driver's weight 150 lb and the weight of additional experimental devices 30 lb, the final weight used in the data analysis is 6520 lb, divided equally on the four single tires. However, to provide certain variations on axle load and vehicle configurations, three of other testing vehicles are also used. All the four used testing vehicles are tabulated in Table 4.

Table 4: Summary of Testing Vehicles in Virginia Experiment

Vehicle	Manufacture	Year	Model	Weight (lb)	Distance between Axles (inch)	Distance between Wheels (inch)	Width of Tire (mm)
1	Chevrolet	1999	Express 3500	6603	160	67.5	245
2	Ford	1997	Taurus LX	3753	108.5	61.5	205
3	GMC	1998	Sierra	4724	132.5	64	225
4	Ford	2001	Escape	3730	103	60.5	235

NOTE: 1 lb = 0.454 kg; 1 inch = 25.4 mm. Weight listed includes the weight of the vehicle, one drivers and one passenger.

PAVEMENT HEALTH STATUS MONITORING

As one of the most important and expensive investments/assets in the modern society, asphalt concrete pavement ages and deteriorates with time as a result of asphalt mixture aging, excessive use, overloading, environmental conditions, and inadequate maintenances. All of these factors contribute to the deterioration process which is very complicated. Various pavement distresses, including cracking, rutting, wear, deflection and so on, are important indicators of pavement performance. In this project, a pavement health monitoring system was developed based on embedded wireless sensing network. The sensing network was designed for pavement health monitoring as an efficient combination of various commercial pavement sensors.

Pavement Mechanical Responses

As shown in Figure 9, four sensors were arranged at the same transverse offset distance to measure various mechanical responses at the corresponding position. The combination of the four sensors were called a sensing group, which includes a load cell, a vertical strain gauge, horizontal strain gauges in longitudinal and transverse plane of traffic. The wandering of vehicle between the sensors in same groups is ignored, and the measured mechanical responses from the same sensing group were treated to be at the same point in transverse plane. All the vertical strain gauges were damaged after five months probably because of the bad environment and excessive load, and the following analysis included only load cells and corresponding horizontal strain gauges.

The responses of strain/stress change with various loading and environmental conditions, for example axle load, temperature, speed, vehicle configuration and so on. The present strain and stress responses in Figure 10 were collected from the left wheel path (A1-A11) during a regular test run.

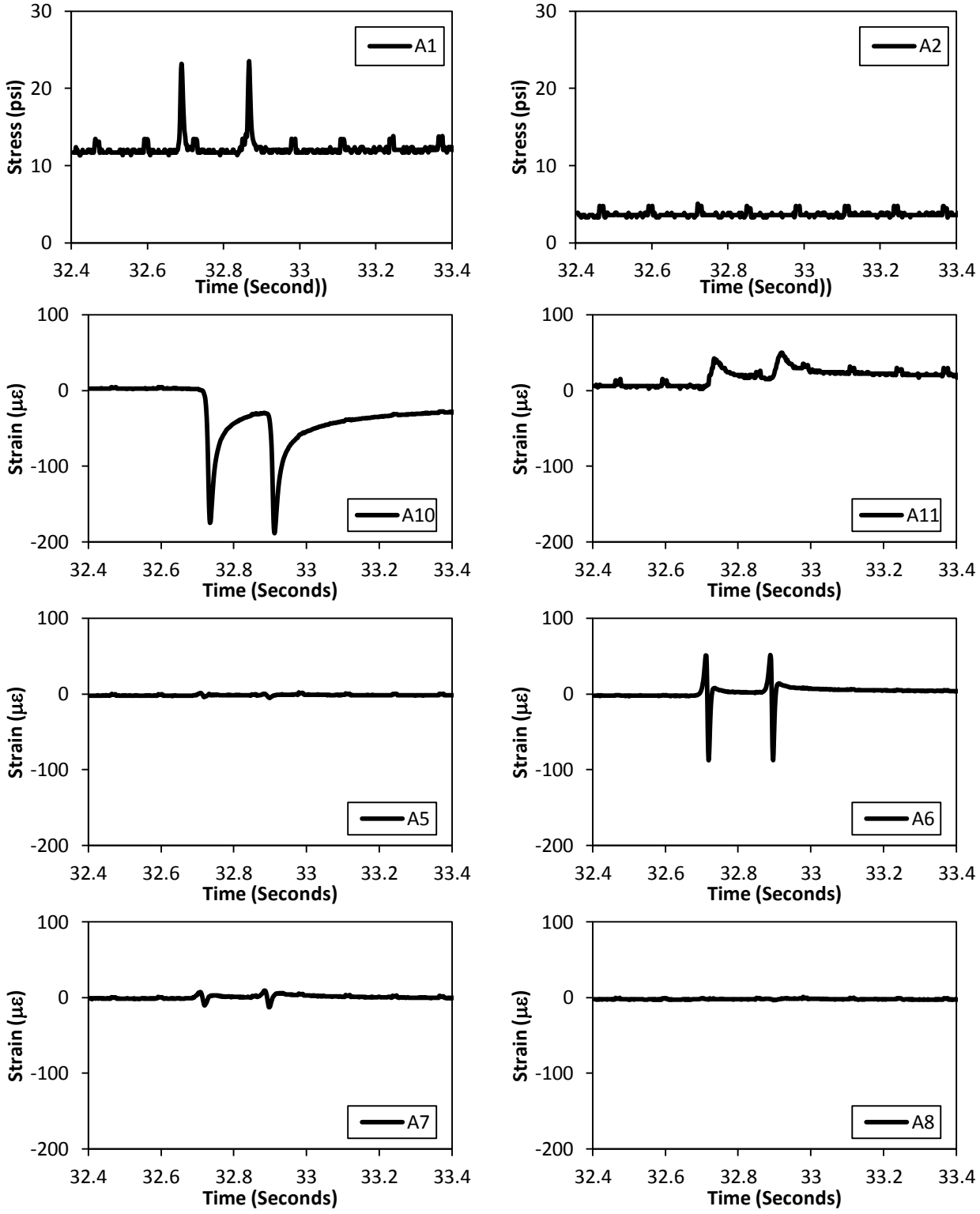
A1
Stress (psi)
Time (Second))
A2
Stress (psi)
Time (Second))
A10
Strain (με)
Time (Seconds)
A11
Strain (με)
Time (Seconds)
A5
Strain (με)
Time (Seconds)
A6
Strain (με)
Time (Seconds)
A7
Strain (με)
Time (Seconds)
A8
Strain (με)
Time (Seconds)

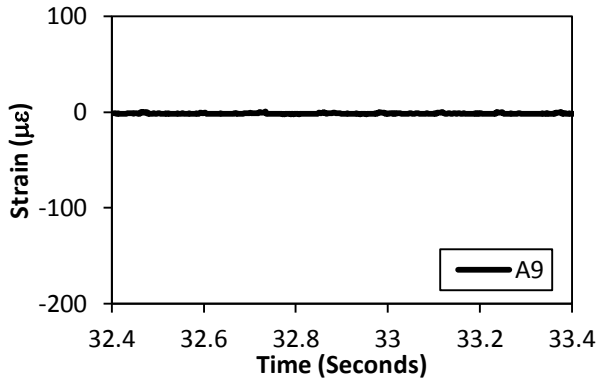

Figure 10 Typical Responses of Strain/Stress Data Collection

As shown in Figure 10, the collected signals are clear and make a lot of sense. The conclusion can be drawn that the front and rear wheel of test vehicle passed the experimental section at the transverse position of A1, A6 and A10, because the mechanical responses from these three sensors are much more obvious than others.

Numerical Simulation

The pavement surface layer of asphalt concrete was treated as linear visco-elastic material, and the complex modulus is dependent on the temperature and loading frequency. With the principle of time temperature superposition, temperature and absolute frequency are combined together to a reduced frequency, and material property only depends on reduced frequency, instead of temperature and absolute frequency separately. The reduced frequency and the reduced time are defined as

$$\omega_R = \omega \times \alpha(T) \qquad \text{Eq.(2)}$$

$$t_R = \frac{t}{\alpha(T)} \qquad \text{Eq.(3)}$$

where ω is the actual loading frequency, $\alpha(T)$ is temperature shift factor, T is temperature, $\omega(R)$ is reduced frequency; t is the actual loading time, t_R is reduced time. Based on the dynamic test results provided by VDOT, the dynamic master curve of the target asphalt concrete

layer under the reference temperature 70°F after placement is shown in Figure 11, together with the shift factors under different temperatures.

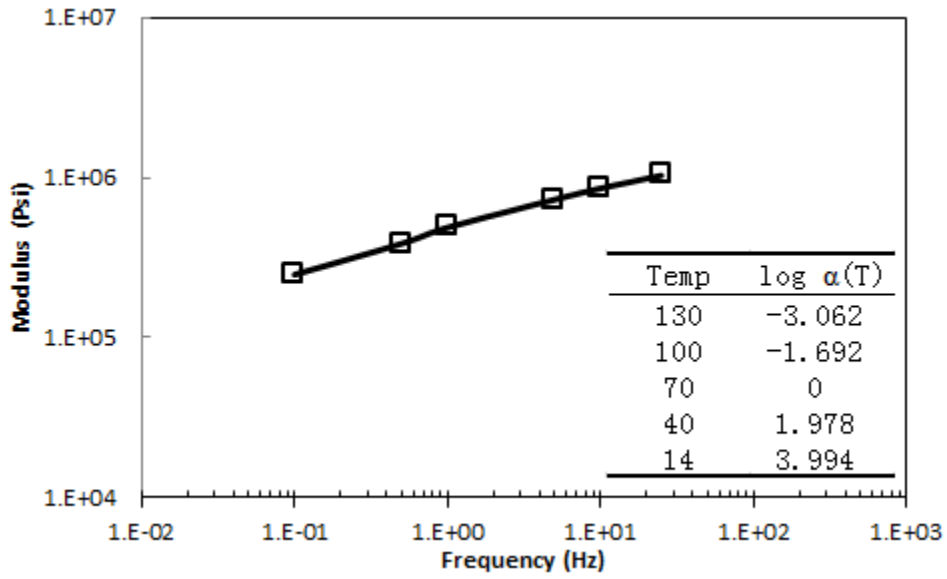

Figure 11 Original Dynamic Master Curve of the Surface Layer

Finite Element Method (FEM) based software ABAQUS was used to conduct mechanical analysis of the pavement section theoretically. Viscoelastic property present in Figure 11 was input for the surface layer of asphalt mixture, and the sub-layers were treated as linear elastic materials. The passing process of single wheel was simulated under the corresponding temperature and loading frequency, as shown in Figure 12. The comparison between the calculated horizontal strain response and field measurements is shown in Figure 13.

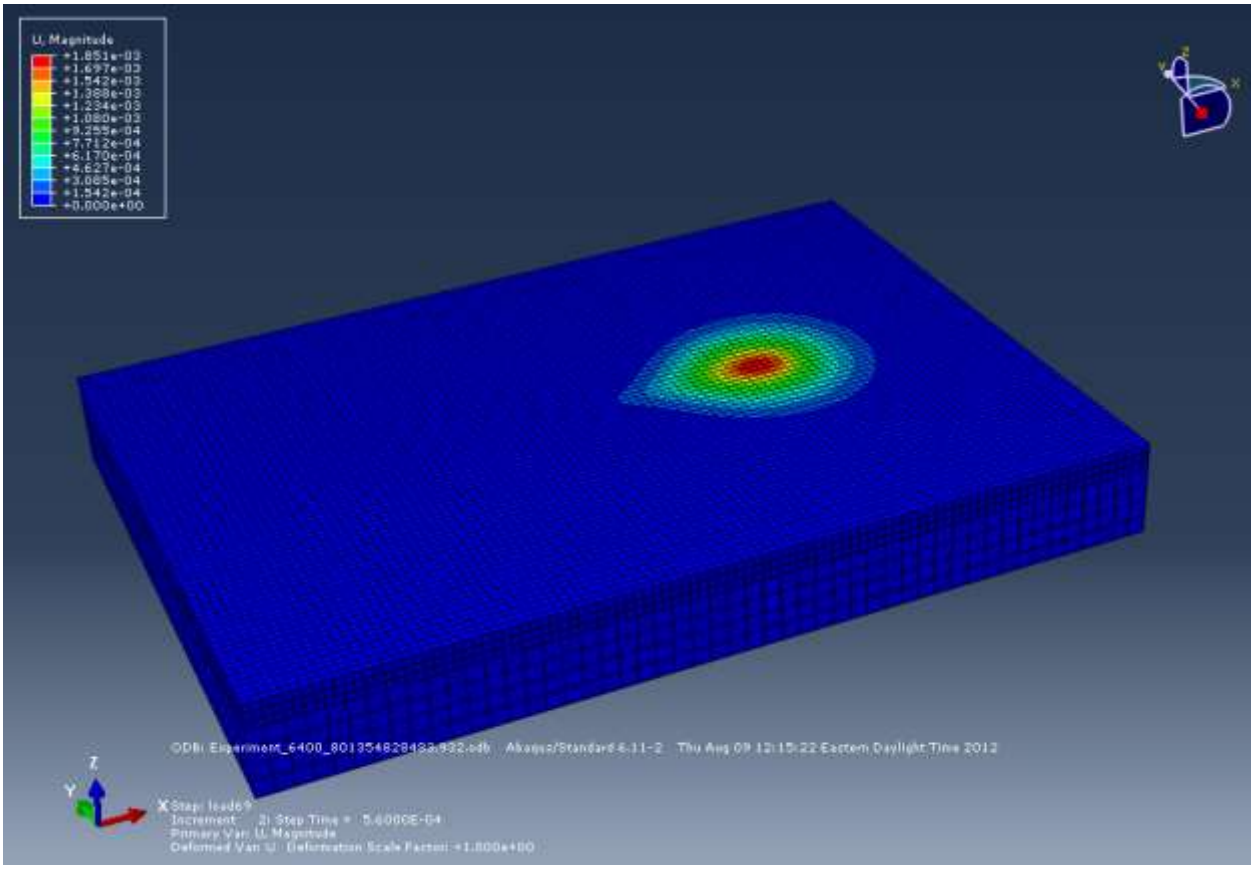

Figure 12 A Numerical Simulation using ABAQUS

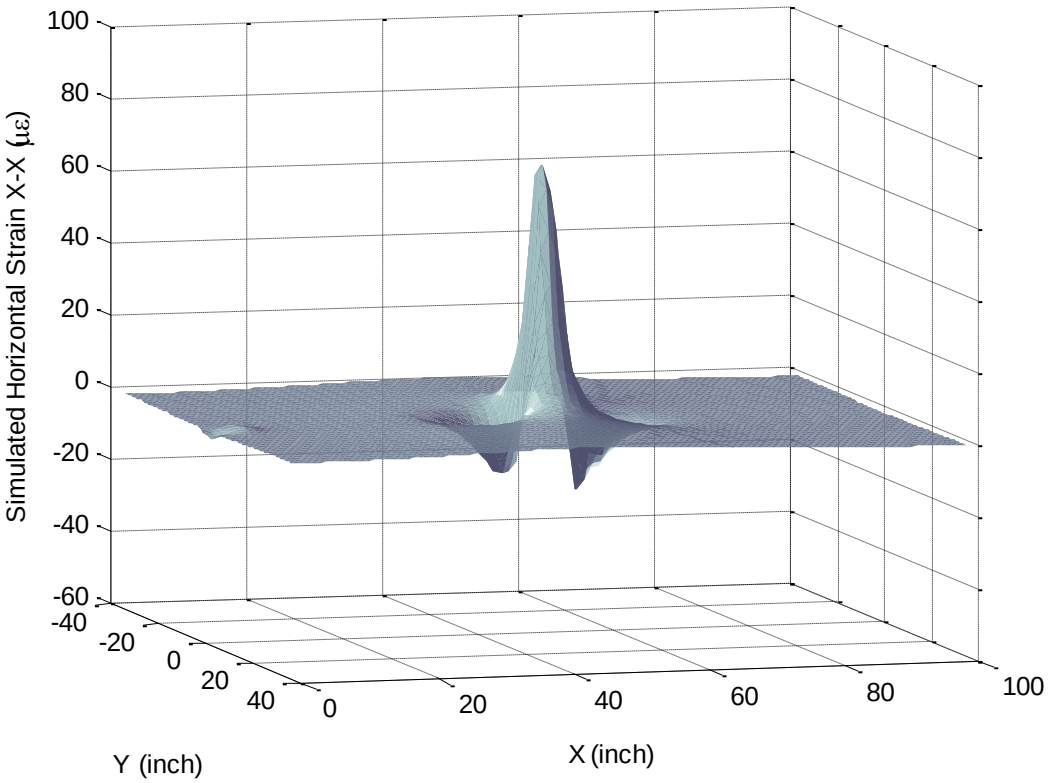
Simulated Horizontal Strain X-X (με)
100
80
60
40
20
0
-20
-40
-60
-40
-20
0
20
40
Y (inch)
0
20
40
60
80
100
X (inch)

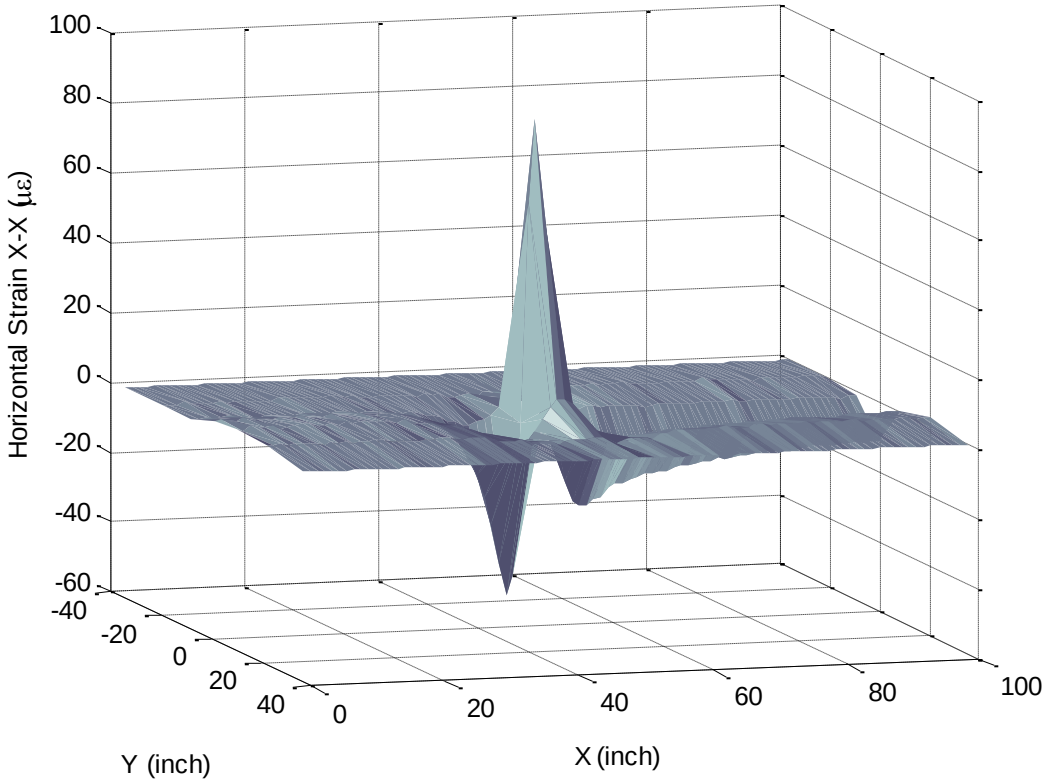

Figure 13 Distribution of Horizontal Strain Response X-X (a. ABAQUS simulation; b. Field Measurement)

X is the horizontal longitudinal direction, parallel to the traffic; Y is the horizontal transverse direction, transverse to traffic

As shown in Figure 13, the simulated strain distribution matches with field strain measurement very well in the shape. Though some error in the magnitude, it is understandable considering the localized pavement structure, variation of material property, and other factors. The precision of 3-dimensional figure in Figure 13(b) is low because only 5 strain gauges were used.

Back Calculation of the Modulus ofAsphalt Concrete Layer

To estimate the structural strength is an important objective of structural evaluation. "For asphalt pavements, it may be expressed in terms of in situ layer elastic moduli, layer thickness, inter-layer bond conditions and anomaly characterization"[73]. Using the proposed pavement health monitoring system, the modulus of asphalt concrete can be back calculated every three or six months based on the adopted policy. The ratio between normal stress in direction A σ_A and

normal strain in direction B ε_B is used to back calculate the elastic modulus of asphalt concrete layer, which is defined as following:

$$R_{AB} = \frac{\sigma_A}{\varepsilon_B} \quad \text{Eq.(4)}$$

The original intention while designing the sensing network is to use collected vertical stress and vertical strain for the modulus back-calculation. However, the vertical strain gauges installed are all out of service due to the harsh environment currently, horizontal strain collected is used instead of vertical strain. The relationship between vertical stress and vertical/horizontal strain was validated by ABAQUS simulation shown in Figure 14.

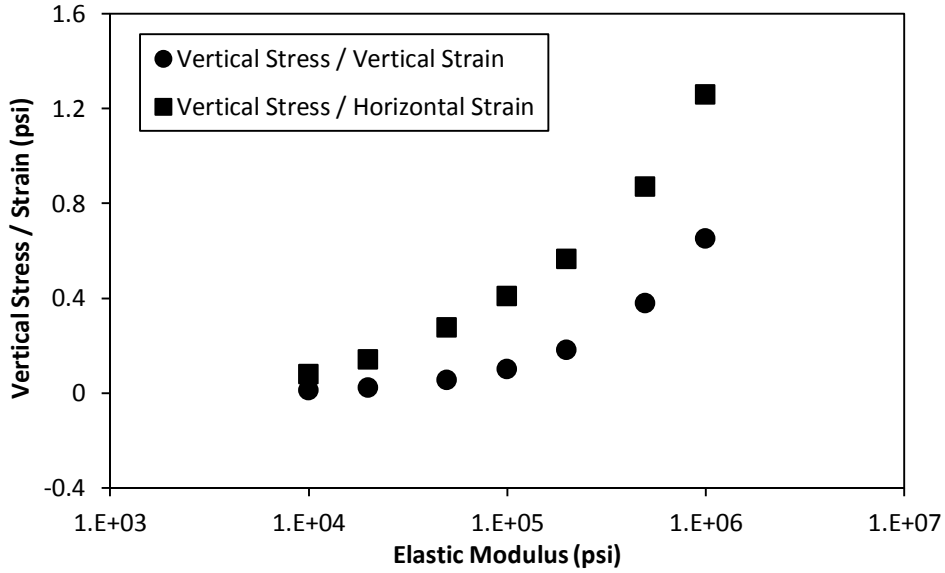

Figure 14 Simulated Relationship between the Parameter R and the Modulus

As shown in Figure 14, the ratio between vertical stress and horizontal strain R_{ZX} is related with the elastic modulus of the asphalt concrete layer, and can be used to back calculate the modulus of the layer.

For example, the responses with testing vehicle passing directly on sensor A6 and A8 are chosen to demonstrate the back-calculation process of pavement dynamic modulus. The parameter R_{ZX}

is calculated from the collected strains and stresses with changing temperature and two speeds, as shown in Figure 15.

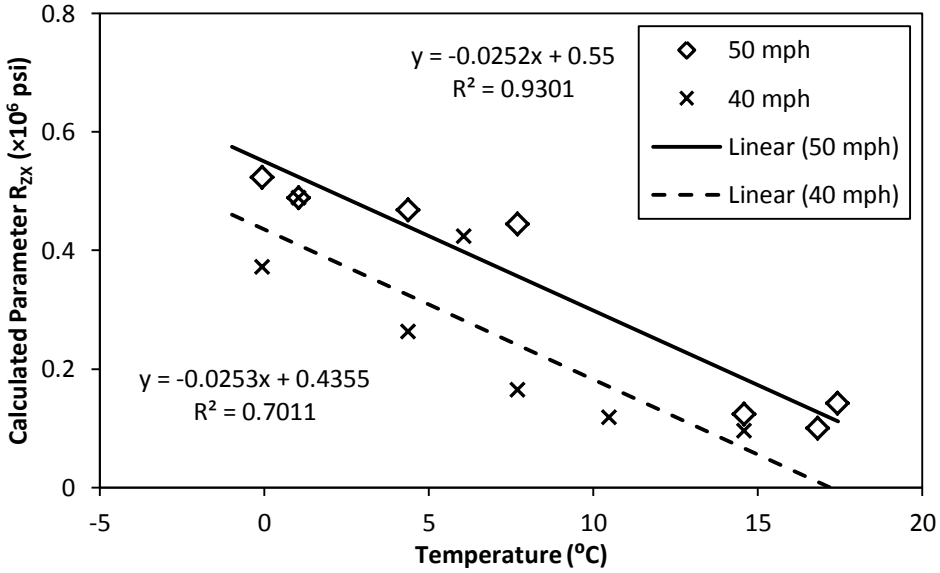

Figure 15 Back Calculated Parameter R_{XZ} with Changing Temperature and Speed

As seen in Figure 15, the calculated parameter R_{ZX}, which was proved to be related to pavement modulus in Figure 14, decrease with temperature and increase with testing vehicle velocity. The trend present makes a lot of sense for asphalt concrete which is usually treated as visco-elastic. The vehicle speed in the finished testing runs was limited to 40 and 50 mph to avoid traffic disruption, and in the actual pavement monitoring system, the testing velocity can be set from 5 mph to 80 mph to build up the dynamic modulus of the experimental section similar as Figure 11.

Pavement Distress Prediction

Based on the intention of this research, various pavement distresses can be predicted based on the pavement responses. However, due to the limited scope and distribution of sensing network in the project, only fatigue cracking and rutting were taken into consideration.

Fatigue Cracking

The cumulative damage concept has been widely used to predict fatigue cracking. It is generally agreed that the allowable number of load repetitions is related to the tensile strain at the bottom

of the asphalt layer. The major difference in the various design methods is the transfer functions that relate the tensile strains in asphalt concrete layer to the allowable number of load repetitions.

For comparison purposes, current Mechanistic-Empirical Pavement Design Guide (MEPDG) fatigue cracking model is used, and the fatigue damage of each tire to the experimental section is calculated by the following functions.

$$N_f = 0.00432C\left(\frac{1}{\varepsilon_t}\right)^{3.291}\left(\frac{1}{E}\right)^{0.854} \quad \text{Eq.(5)}$$

$$C = 10^M \quad \text{Eq.(6)}$$

$$M = 4.84\left(\frac{V_b}{V_a + V_b} - 0.69\right) \quad \text{Eq.(7)}$$

Where N_f = the allowable number of load repetitions for fatigue cracking; ε_t = the tensile strain at the critical location, which is the bottom of asphalt concrete layer; E = the stiffness of asphalt mixture; V_b = the effective binder content (8.4%) and V_a = the air voids of the asphalt mixture (7.4%).

To calculate the fatigue cracking damage brought to the pavement by each run, Eq.(5) can be converted as following.

$$D_{fc} = 231.48\frac{1}{C}(\varepsilon_t)^{3.291}(\mathrm{E})^{0.854} \quad \text{Eq.(8)}$$

where D_{fc} is the fatigue cracking damage brought by each passing vehicle to the pavement section. In the target pavement monitoring system, the parameter $D_{fc,i}$ can be calculated after each passing vehicle, and added into the total D_{fc} as an index of fatigue cracking. When D_{fc} equals to 1, theoretically the pavement section is totally damaged because of fatigue cracking.

Rutting

Permanent deformation is another factor for flexible pavement design and maintenance. "With the increase in traffic load and tire pressure, most of the permanent deformation occurs in the upper layer rather than in the subgrade"[74]. Since only the strain in the asphalt concrete layer is measured in the experiment, then the rutting depth calculated in the paper is only for the asphalt concrete layer of the experimental sections.

The Mechanistic-Empirical Pavement Design Guide (MEPDG) rutting model is used to estimate the rutting depth of experimental sections. This model is derived from statistical analysis of the relationship between plastic and elastic compressive strain in experiments.

$$\frac{\varepsilon_p}{\varepsilon_r} = k_1 \cdot 10^{-3.4488} T^{1.5606} N_r^{0.479244} \quad \text{Eq.(9)}$$

where $\varepsilon_p =$ accumulated plastic strain at N repetition of load; $\varepsilon_r =$ resilient strain of the asphalt material; $N_r =$ number of load repetitions; $T =$ Pavement Temperature, and k_1 is the function of total asphalt layer(s) thickness (H_{ac}) and depth to computational point, as defined in the functions below.

$$k_1 = (C_1 + C_2 \cdot depth) \cdot 0.328196^{depth} \quad \text{Eq.(10)}$$

$$C_1 = -0.1039 \cdot H_{ac}^2 + 2.4868 \cdot H_{ac} - 17.342 \quad \text{Eq.(11)}$$

$$C_2 = 0.0172 \cdot H_{ac}^2 - 1.7331 \cdot H_{ac} + 27.428 \quad \text{Eq.(12)}$$

Then the overall permanent deformation can be computed as sum of permanent deformation for each individual sub-layer.

$$PD = \sum_{1}^{NS} \varepsilon_p^i \cdot h^i \quad \text{Eq.(13)}$$

where PD = pavement permanent deformation; NS = number of sub-layers; ε_p^i = total plastic strain in sub-layer i; and h_i = thickness of sub-layer i.

In this project, all the sensors were installed at the same depth, and the whole asphalt concrete layer was treated as one sub-layer, and 12.5 mm rutting depth was used as a failure criterion $PD_{failure}$. Then the rutting damage induced by each vehicle can be calculated based on the allowable number of load repetition for vertical rutting depth.

$$D_r = \frac{1}{N_r} = \left(k_1 \varepsilon_r \frac{h}{PD_{failure}}\right)^{2.086620} T^{3.256379} 10^{-7.196335} \quad \text{Eq.(14)}$$

where D_r is the rutting damage brought by each passing vehicle to the pavement section. D_r can be computed for each passing axle and summed up as an index of rutting depth. When D_r equals to 1, theoretically the section is totally damaged because of vertical rutting.

Health Monitoring System design

According to the studies above, it is feasible and practical to develop a pavement health monitoring system based on the instrumented sensing network. The prototype of this monitoring system is present in Figure 16.

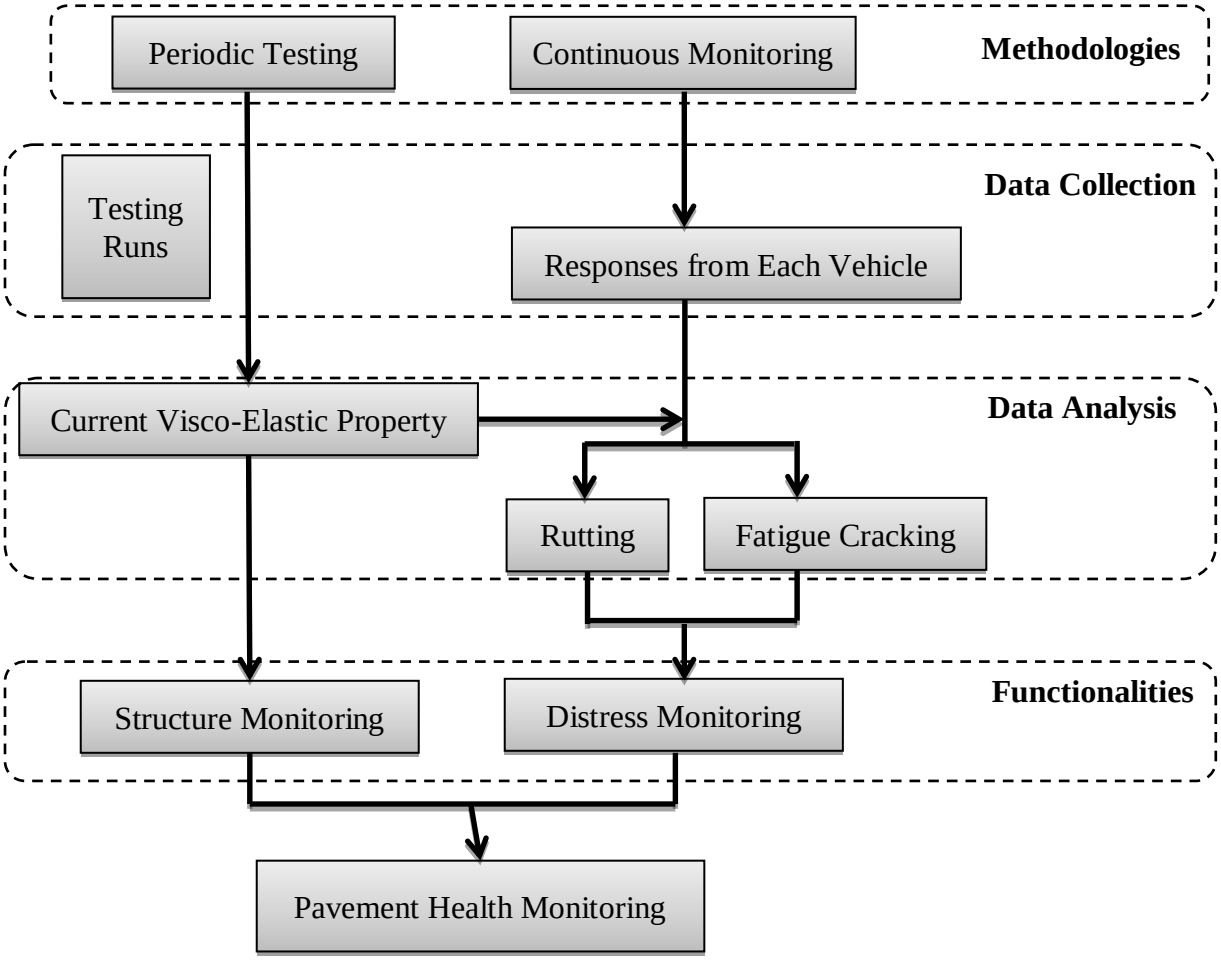

Figure 16 Diagram of the Pavement Health Monitoring System

As shown in Figure 16, the routine monitoring contents of this system include periodic testing and continuous monitoring. The periodic testing can be conducted every year or other fixed period with testing runs, and the back-calculated dynamic modulus can be used to evaluate the health status of the pavement structure. At the same time, the strain/stress responses in pavement are collected in continuous real-time monitoring for each passing vehicle. Pavement distresses can be predicted with the collected mechanical response with different pavement distress prediction model, used for pavement management system.

Summary

This paper illustrates the great potential of complete pavement health monitoring system using common commercial pavement sensors used to design wireless sensing network. Four

measurements from different pavement sensors were taken including temperature, moisture, strain and stress. Up to now, the collected responses are proved to be clear and reasonable, and ready for further analysis. The FEM simulation of strain distribution using visco-elastic material model for asphalt concrete was shown to agree well with those experimental measurements at a reasonable range of error. The ratio between vertical stress and longitudinal horizontal strain was demonstrated to be related to the strength of pavements, and can be used for the back-calculation of pavement modulus. At the same time, the MEPDG fatigue cracking and rutting models were written into the damage brought by each passing vehicle, and taken into the prediction of pavement distresses for the health monitoring system. In the end, a working prototype of pavement health monitoring system was set up to clarify the routine monitoring content, data analysis process and final functionalities.

In general, this monitoring system is based on the in-situ pavement sensors, and has a high feasibility and practical value to be carried out for pavement management and research purposes because of the following advantages:

- ✓ Low cost for installation and maintenances;
- ✓ Taken the actual strain response in pavements into the distress prediction;
- ✓ Valuable for the validation of pavement distress models;
- ✓ Can be integrated with other pavement instrumentation (Weigh-In-Motion, Energy Harvesting and Traffic Classification systems) easily.

TRAFFIC INFORMATION BACK-CALCULATION

Reliable information collection of traffic flow is important for Intelligent Transportation Systems (ITS) to make timely decisions on traffic signal timing and optimization. Based on different purposes, the target information of traffic flow for a specific section might include speed, traffic volume, classification, and axle load. In recent decades, lots of efforts have been devoted to improve the information collection of Intelligent Transportation System with various technologies.

It is critical for Intelligent Transportation System (ITS) to provide accurate forecasts of traffic volumes in real-time [75]. Various methodologies and techniques have been utilized to forecast traffic volumes, including short-term and long-term forecasting [76]. Long-term forecasting targets at monthly or yearly volume for planning, design, and management of highway networks, and highway agencies usually use permanent traffic counters (PTCs) at highway sections to record traffic volume continuously[77]. Short-term forecasting focuses on predicting traffic flow changes in short time (15-30 minutes) with various roadway sensors.

The speed of traffic flow is directly related to travel time, which is essential in the traffic condition evaluation and management. In addition, speed is also a criterion for traffic congestion, which has become one of the major problems in metropolises[78]. Different sensing technologies have been applied to the speed estimation of vehicles, including image processing[78, 79], Bluetooth sensors[80] and so on.

With the development of transportation socialization, traditional pavement monitoring systems have been integrated with other monitoring systems, such as Weigh-in-Motion (WIM) and Traffic Classification system. Weigh-in-Motion is to obtain the weight of a vehicle while the vehicle is moving. Traffic classification is to measure configuration parameter of passing vehicles with detector, and classify them for traffic analysis and management. It plays an important role in Intelligent Transportation System for the analysis and management of traffic flow. WIM systems and vehicle classification system mentioned above, together with vehicle speed measurement have been combined together as traffic data collection system by some transportation agencies [65-68].

An integrated transportation monitoring system was developed at Virginia Tech, which can monitor the health status of the pavement and collect the speed, weight and configuration of the traffic simultaneously. This paper introduces the back calculation method used to count traffic and estimate the weight, speed and configuration parameters of passing vehicles with mechanical responses from in-pavement strain/stress sensing device, which also serve for pavement health monitoring.

Gaussian Function

To back calculate various parameters from traffic , it is necessary to have the strain and/or stress distribution in the cross-section of the pavement. As shown in Figure 9, ten horizontal strain gauges were placed in a transverse line crossing the two wheel path separately. When a vehicle passes by, every gauge records a strain trace corresponding to its location. Peak response is extracted from each trace for the following analysis. Without additional instructions, all the strain mentioned later refers to the measurement from sensor A5-A9 and B5-B9.

Considering only one tire moving over the instrumented section, the viscoelastic dynamic process is modeled with the Finite Element Method based software ABAQUS. The maximum strain response corresponding to each tire of the vehicle are measured, and compared with the corresponding numerical simulation in Figure 17.

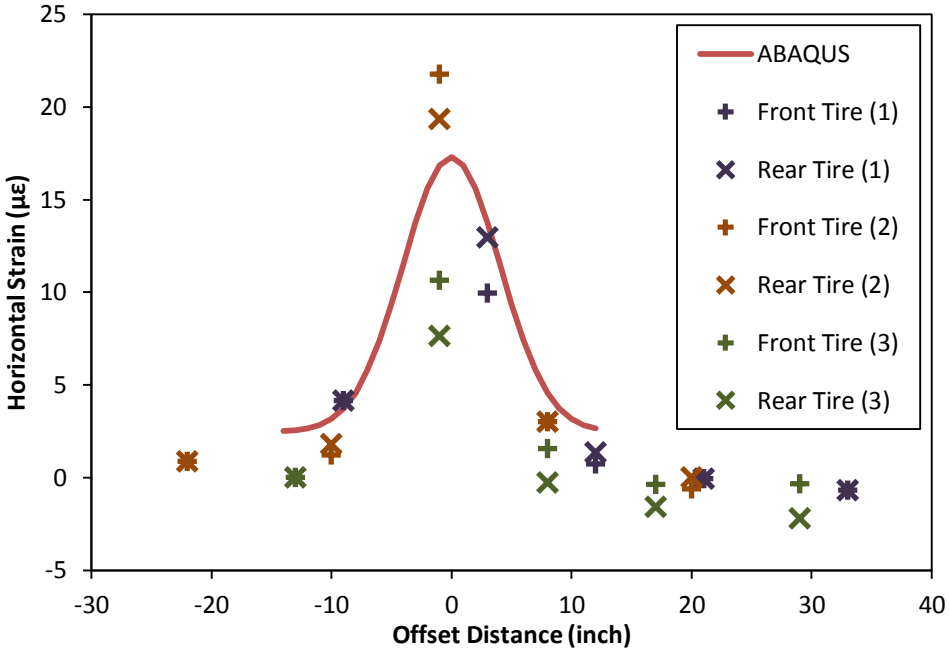

Figure 17: Comparison between ABAQUS Calculation and Measured Horizontal Strain.

As shown in Figure 17, the ABAQUS calculated responses match the actual measurement well with some deviation. Considering the changing temperature, and the uncertainty of dynamic process simulation, the ABAQUS model works quite well and can be treated as the theoretical basis in the following analysis.

Since the spatial distribution of the horizontal strain looks similar to normal distribution, Gaussian function is adopted to model the spatial distribution of horizontal strain. With two additional parameters, A and b, the original expression of normal distribution is modified to Eq.(15).

$$\varepsilon = \frac{A}{\sigma\sqrt{2\pi}} e^{-\frac{1}{2}\left(\frac{x-\mu}{\sigma}\right)^2} + b, \qquad \text{Eq.(15)}$$

where ε represent the target horizontal strain; A, μ, σ, and b are all the parameters which are going to be simulated by the SOLVER in EXCEL. These parameters have their specific meanings in the strain distribution of pavement:

- μ -- The distance between the center of the strain distribution and the reference line in the transverse plane, related to the wandering position of the passing tire;
- σ -- The width of the strain spread in pavement, related to the width of the passing tire;
- b -- The up and down shift of the whole strain distribution;
- A -- The area under the strain distribution curve when b=0.

As shown in Figure 17, the whole structure, not only the area under the tire, withstands the total load. For simplification and efficiency, it is assumed that only the area [μ-3σ, μ+3σ] contribute to the load standing. Then another two integrated parameter L and s are defined as:

$$L = A + 6\sigma b, \qquad \text{Eq.(16)}$$

$$s = b / A, \qquad \text{Eq.(17)}$$

where L represents the total area under the strain distribution curve between μ-3σ and μ+3σ, and is related to the load applied by the passing tire. The Gaussian distribution function can be expressed as:

$$f = \frac{L}{\sqrt{2\pi}\sigma(1+6\sigma s)} e^{-\frac{1}{2}\left(\frac{x-\mu}{\sigma}\right)^2} + \frac{Ls}{1+6\sigma s}, \qquad \text{Eq.(18)}$$

Replacing A and b with L=A+6b and s=b/A makes L the only parameter that represents the passing load. In this expression, lots of useful information about the passing vehicle can be obtained. To validate these assumptions, single tire passing process is modeled in ABAQUS with different loading conditions. Each predicted strain distribution is simulated with Gaussian function separately, and the parameters are summarized in Table 5.

Table 5: Calculated Parameter of Gaussian Function under Various Loading Conditions in ABAQUS (18.1°C)

Series	Load (lb)	Width of Loading Area (inch)	Offset Distance (inch)	L	σ	μ	s

1	5600	4	0	184.1	4.044	0.001	0.01644
2	6400	4	0	210.4	4.044	0.001	0.01643
3	7200	4	0	236.6	4.044	0.001	0.01643
4	6400	3	0	211.9	3.795	0.003	0.01741
5	6400	5	0	210.8	4.293	0.002	0.01460
6	6400	4	-1	209.9	4.010	-1.001	0.01709
7	6400	4	1	210.7	4.099	1.002	0.01514

Offset Distance – the transverse distance between the centerline of the loading area to the middle of the wheel path. It is positive when wheel is on the left side of wheel path.

When the tire passes the experimental section at different wandering position (series 2, 6 and 7), the simulated parameter μ changes correspondingly, and the difference of other 3 parameters is neglectable. So the parameter μ might indicate the offset distance of the passing tire to the reference line.

Based on the comparison of series 2, 4 and 5, when the width of the loading area increases with other parameters constant, σ is the only parameter that has an obvious response. It can be assumed that σ represents the width of the loading area in the simulation.

According to the simulated parameter of series 1, 2 and 3, L increase linearly with load, and the other 3 parameters σ, μ, and s keep constant. The relationship between L and load is very important for weight back calculation.

As described above, the simulated parameters are related to loading condition parameters in numerical simulation. To verify these assumptions, back calculations of loading conditions are made to collected strain responses and compared with the static measurement in the following section.

Back calculation procedure

The speed and distance between axles can be calculated via traces obtained from different sensors. For the other aspects, including offset distance, width of tire, wheel load and the distance between wheels, Bell Curve Model is necessary with the prerequisites of following procedures.

- The five strain gauges across the wheel path record strain traces via time for each wheel of passing vehicles;
- Five peak points are extracted from traces and constitute a distribution curve for the wheel;
- Bell model is used to analyze each distribution curve in transverse plane and four parameters are obtained, which is used for the following back calculation.

Such procedures were repeated in the experiment, the measured speed and the simulated parameters of each run are summarized in Table 6. These parameters can be used for back calculation of vehicle configuration and axle load, as described in the following sections.

Table 6: Measured Speed (Speed Gun) and Simulated Parameters of Bell Curve Model (35~36°C)

Run	Vehicle	Speed (mph)	Left Tire				Right Tire			
			L	σ	μ	s	L	σ	μ	s
1	1	42	688	5.43	-4.48	0.0013	749	4.21	-9.96	-0.0014
			774	5.62	-6.15	0.0007	826	4.59	-11.74	-0.0015
2	1	43	1080	4.69	7.68	-0.0010	608	4.82	4.01	-0.0017
			985	5.26	7.21	-0.0017	590	5.20	2.60	-0.0026
3	1	44	700	4.73	-3.42	-0.0003	840	4.02	-9.97	-0.0004
			640	4.94	-4.96	0.0001	750	3.89	-9.67	-0.0017
4	2	40	863	3.55	0.22	0.0039	556	4.00	3.10	0.0003
			425	2.60	1.12	0.0085	227	4.00	1.85	-0.0061
5	2	50	776	3.29	2.55	0.0045	655	2.90	5.16	0.0059
			417	3.03	2.81	0.0049	238	2.78	4.70	-0.0053
6	2	52	696	2.65	-4.29	0.0039	612	2.39	-3.93	0.0003
			377	2.34	-4.48	0.0069	328	2.17	-4.16	-0.0022
7	3	48	NA	NA	NA	NA	NA	NA	NA	NA
8	3	47	993	5.11	-9.56	0.0010	472	4.23	-9.56	-0.0004
			762	5.03	-9.91	0.0009	290	4.37	-10.00	-0.0023
9	3	48	610	3.99	-4.25	0.0037	733	4.22	-5.43	0.0002
			404	3.55	-4.53	0.0041	449	3.79	-6.43	-0.0010
10	4	53	544	4.87	-1.52	0.0014	311	4.78	-0.48	-0.0019
			282	4.33	-3.70	0.0040	262	5.19	-1.42	-0.0001
11	4	49	617	4.34	-0.97	0.0031	424	4.60	-1.41	-0.0003
			328	3.48	-3.33	0.0072	278	4.59	-0.62	-0.0025
12	4	40	728	3.64	-6.96	0.0040	416	3.30	-6.45	-0.0002
			606	4.68	-9.45	0.0027	418	4.67	-8.77	0.0025

NOTE: NA = not applicable, the signal is out of sensing range due to a big offset; 1 mph = 1.6 km per hour.

Traffic Volume

Traffic volume can be monitored with the combination of signals from the five horizontal strain gages distributed in each wheel path. A simple but efficient way can be used to count the number of passing vehicle based on the sum of strain responses. The sum of collected strain responses in transverse plane can be calculated as:

$$SS = A_5 + A_6 + A_7 + A_8 + A_9 \text{ or } B_5 + B_6 + B_7 + B_8 + B_9 \tag{5}$$

where A_i and B_i represents the horizontal strain gage installed in wheel paths, as labeled in Figure 9. As an index of traffic flow, SS changes obviously corresponding to each axle of load on pavements, as shown in Figure 18.

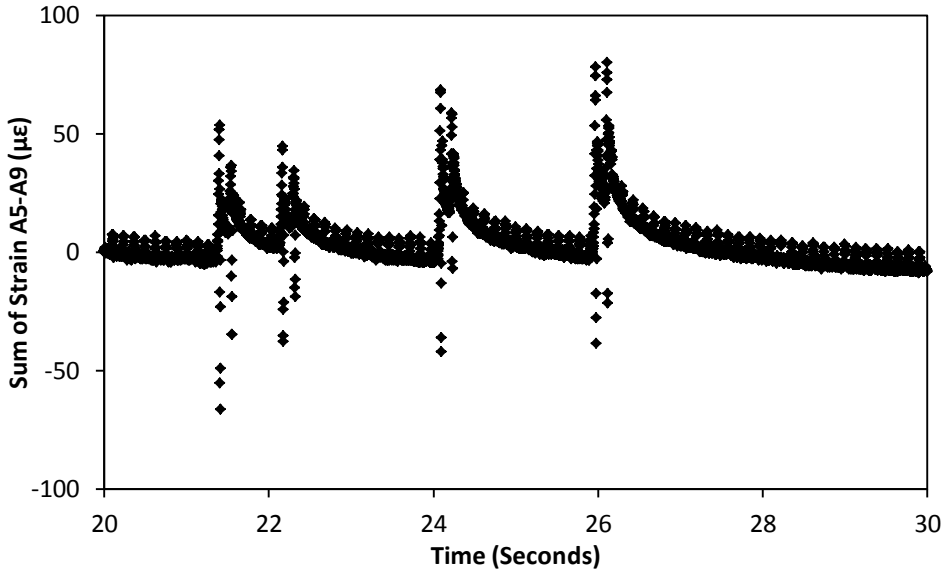

Figure 18 Sum of Strains A5-A9 in 10 seconds

Eight visible fluctuations of SS are present in Figure 18, which match well with the eight axles of four passing vehicles in the experiment as recorded in the corresponding video. With this back calculation method, the number of axles and vehicles can be easily obtained at the same time of the traffic flow with a very low calculation cost. Since the horizontal strain gages A5-A9 cover the whole wheel path, all the passing vehicles in this lane can be recorded without considering their positions.

Speed

The vehicle speed is a necessary parameter for the monitoring system because that the speed of the passing vehicle can affect the visco-elastic properties of the pavement, and then the strain-stress relationship as a result. At the same time, it is also an important objective for the traffic monitoring because the speed of the traffic can be an index for both safety control and the efficiency of the traffic flow. There are two methods present in this section to calculate the speed of the passing vehicle.

If the model of the passing vehicle is known, then the distance of the wheels is fixed, and then the speed can calculated with the time interval of the two fluctuations caused by the front and rear tires separately.

$$SP = \frac{D_{Axles}}{T_2 - T_1} \qquad \text{Eq.(19)}$$

where SP is the speed of the passing vehicle; D_{Axles} is the longitudinal distance between axles; T_1 and T_2 are the corresponding time coordinates for front and rear fluctuations. This equation is theoretically accurate, and proved in our experiment. The signal present in Figure 19 is collected for a passing vehicle, whose speed is controlled at 50 mph manually.

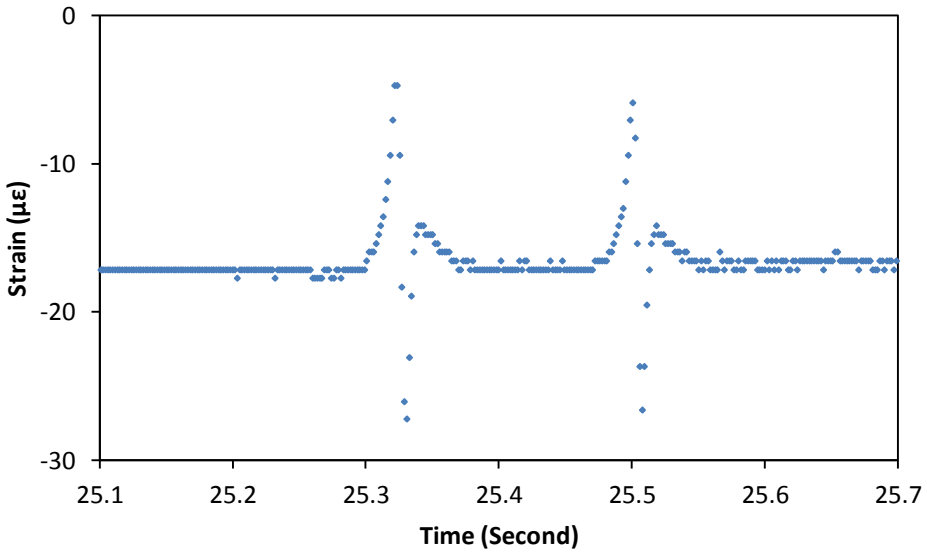

Figure 19: Signal Sample Collected in an On-Site Experiment

Data collected from B5 on June 6 2012.

The back calculated speed matches with the speed gun perfectly. This method is very easy and convenient, and feasible when only one or two traces of strain or stress are captured. However, the disadvantage is also very obvious, because the distance between the wheels has to be known.

In fact, the models of the running vehicles on the pavement are unknown to the researchers, and the first present method can't be used. In this case, the velocity can be calculated with the traces of different sensors. Since the sensors are installed with different x (longitudinal coordinates, in the direction of traffic), the velocity can be calculated with the time interval between different sensors. With two sensors installed along the direction of traffic, the velocity can be obtained by dividing the distance with time interval of the two sensors, as shown in Eq.(20).

$$SP = \frac{D_{ij}}{T_j - T_i} \qquad \text{Eq.(20)}$$

where SP is the speed of the passing vehicle; D_{ij} is the longitudinal distance between the sensor i and j; T_i and T_j are the corresponding time coordinates for the same peak point in this fluctuation.

For example, sensor B1 and B10 are placed along the traffic direction, and the time interval between their fluctuations, shown in Figure 20, can be used to calculate the speed of the vehicle. System error might exist because of the installation, and can be adjusted by a system constant. Lots of runs have been made, and the back calculated speeds are compared to the measurement of speed gun in Figure 21 for statistical analysis.

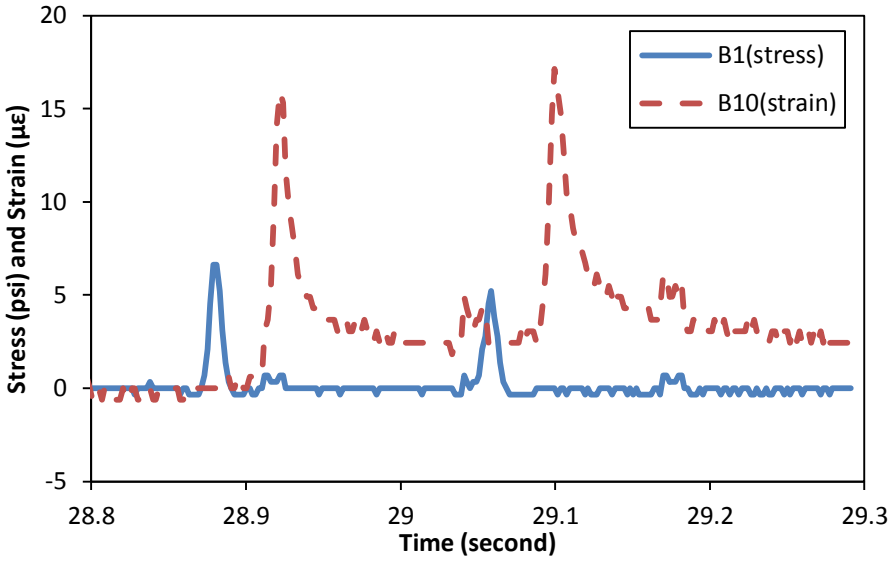

Figure 20: Responses of B1 and B10 Gaugesfor the Same Run.

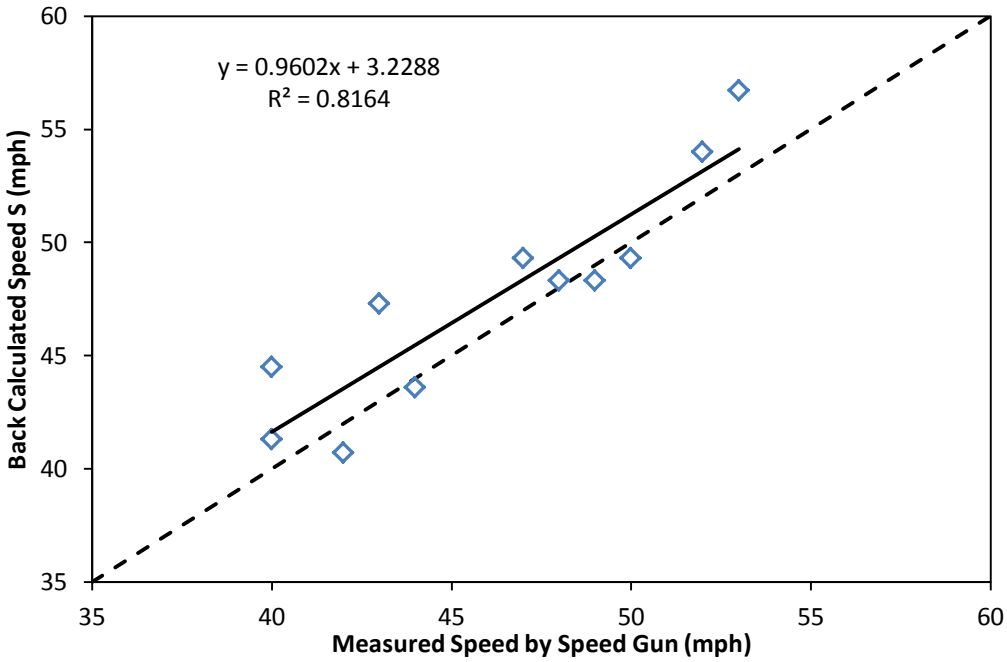

Figure 21: Back Calculated Speed Compared versus Measurement of Speed Gun.

NOTE: 1 mph = 1.61 km per hour

The calculated speed matches well with manual measurement with a speed gun. The deviation is understandable because the speed of actual traffic keeps changing all the time, and error exists in the speed reading which is based on personal judgments. Other sources of error include the

sensor installation, the streaming frequency of data collection, measuring error of the speed gun and so on.

Distance between Axles

With the speed of the passing vehicle known, the distances between the front and rear axles can be calculated with Eq. (21).

$$D_{axle} = SP \times (T_r - T_f) \quad \text{Eq.(21)}$$

where D_{axle} is the distance between the front and rear axles of the vehicle; T_r and T_f are the time of the maximum tensile strain caused by rear and front tires.

The distance between axles are calculated for all the testing runs, and compared to the static manual measurements in Figure 22.

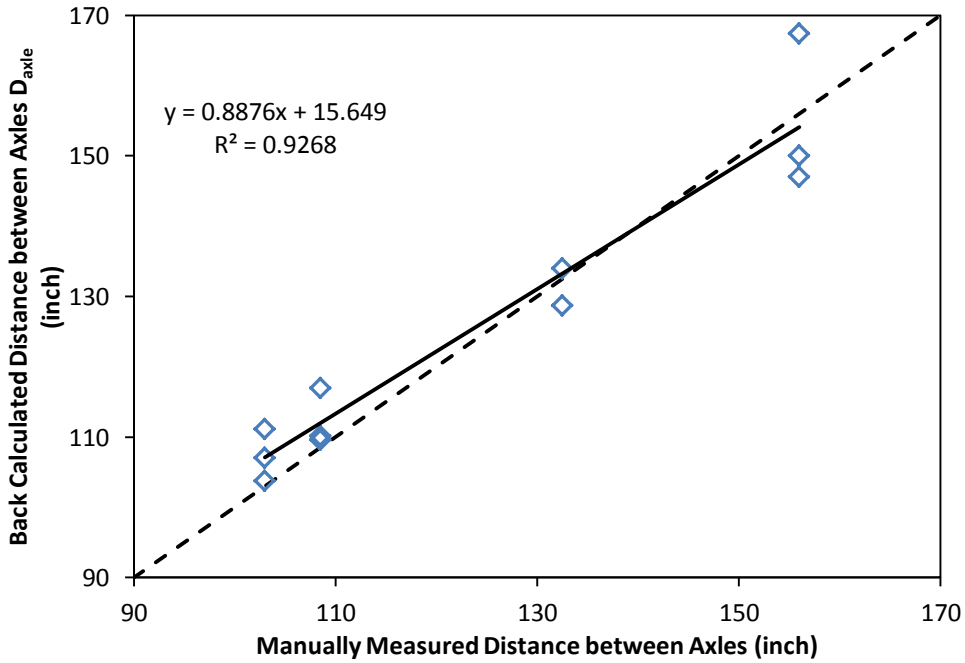

Figure 22: Back Calculated Distance Between Axles.

NOTE: 1 inch = 25.4 mm.

From the comparisons in Figure 22, the back calculated distance between axles is very accurate, and its distribution is very similar with back calculated speed. The dependency is understandable, because the calculation process is based on the speed results.

Wandering Position

Bell Curve model is used in simulation based on the distribution of longitudinal horizontal strain, as shown in Figure 23. According to the simulated parameter μ, the tire passes the experimental section approximately 12 inch right of the centerline.

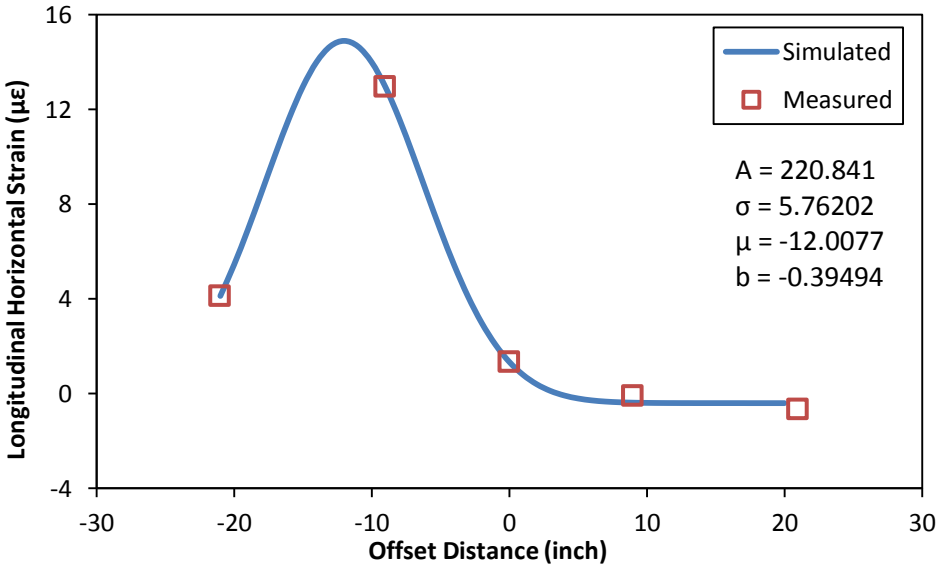

Figure 23: Simulation with Bell Curve Model for a Wheel Load.

NOTE: 1 inch = 25.4 mm.

The wandering position calculated here might not be a parameter people care about, however it is very important for the back calculation of vehicle configuration and axle load, which are going to be described in the following sections.

Distance between Wheels

Knowing the wandering position of the two wheels, the distance between wheels can be calculated as:

$$D_{wheel} = 0.5WL + \mu_A - \mu_B, \qquad \text{Eq.(22)}$$

where D_{wheel} is the distance between the two wheels on the same axle; WL is the width of the lane, which is usually 144 inch; μ_A and μ_B is the calculated wandering position from gauge group A and B separately.

To verify the back calculation, the distance between the outer edges of the wheels is measured manually for each involved vehicle, as well as the distance between the wheels' centers (Table 4). The measurements are compared to the back calculation results in Figure 24.

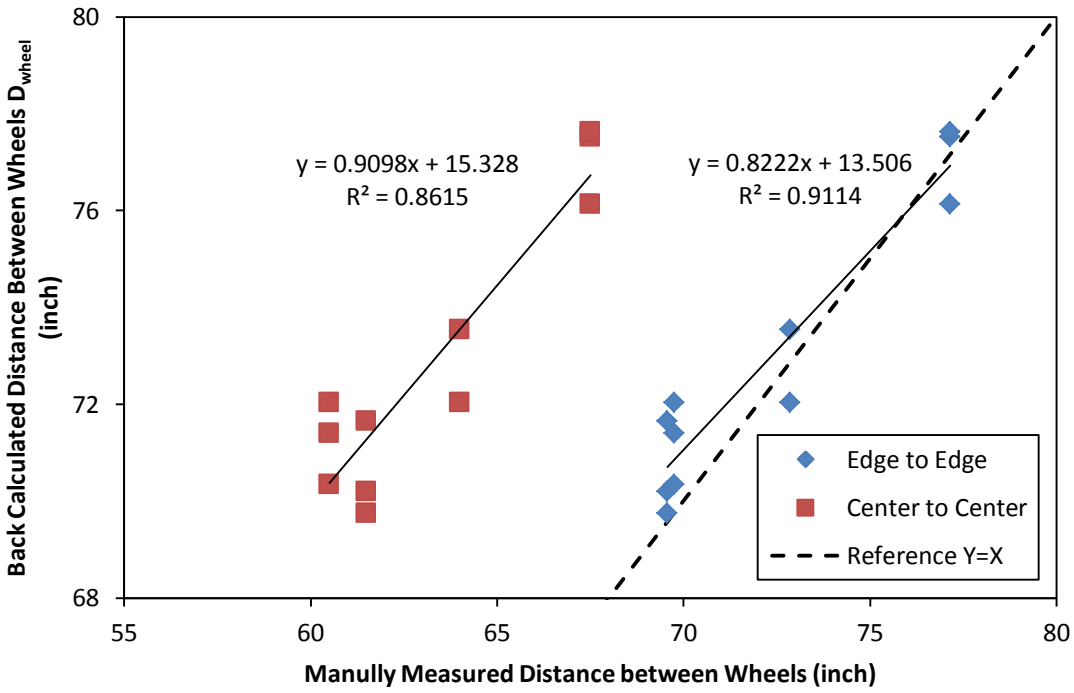

Figure 24: Back Calculated Distance between Wheels.

In the back calculation, the center of the bell shaped fluctuation corresponds to the peak strain response in pavement, and the distance between the left and right centers is called the distance between wheels. As shown in Figure 24, the back calculated distances between wheels match with the measurement between outer edges of the tires, not the centers of the tires. It is because

that the pressure distribution under the tire is not uniform, and the outer edge applies the most pressure to pavement.

Width of the tire

The parameter σ of the bell curve model, which controls the shape of the bell curve, is assumed to be correlated with the width of the tire. The calculated parameter σ presents a second order polynomial relationship with the corresponding tire width in Figure 25..

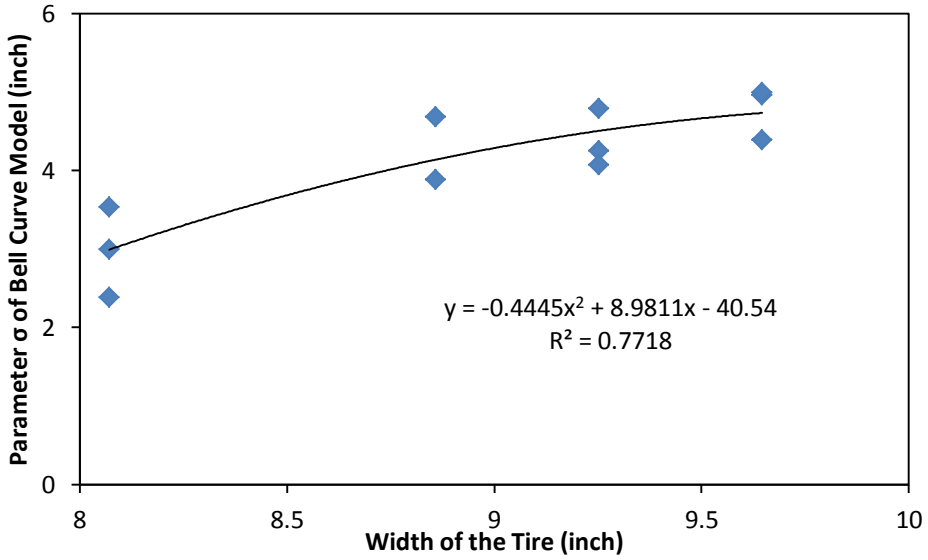

Figure 25: Back Calculated Parameter σ and the Width of Corresponding Tire.

As shown in Figure 25, the simulated parameter σ has a relationship with the actual width of tire. As a result, parameter σ can be used to estimate the tire width for passing vehicles. There is some variation in Figure 25 because the number of sensors in transverse plane is limited. At the same time, the contact area between tire and pavement changes with speed and temperature, which makes the estimate of tire width pretty difficult.

Weight

The weight of the passing vehicle is one primary objective of this method, and the monitoring system is expected to work as a Weigh-In-Motion system. As assumed in Bell Curve model, the

parameter L defined in Eq. (2) represents the passing load, and increases linearly with increasing load when the other loading condition and environmental condition keep constant.

In one experiment, the temperature of pavement changes in the small range between 35 and 36 Degree Celsius which is neglected in the comparison. The sum of back calculated parameter L ($\sum L$) is calculated for each passing vehicle, and summarized in Figure 26 with the corresponding weight.

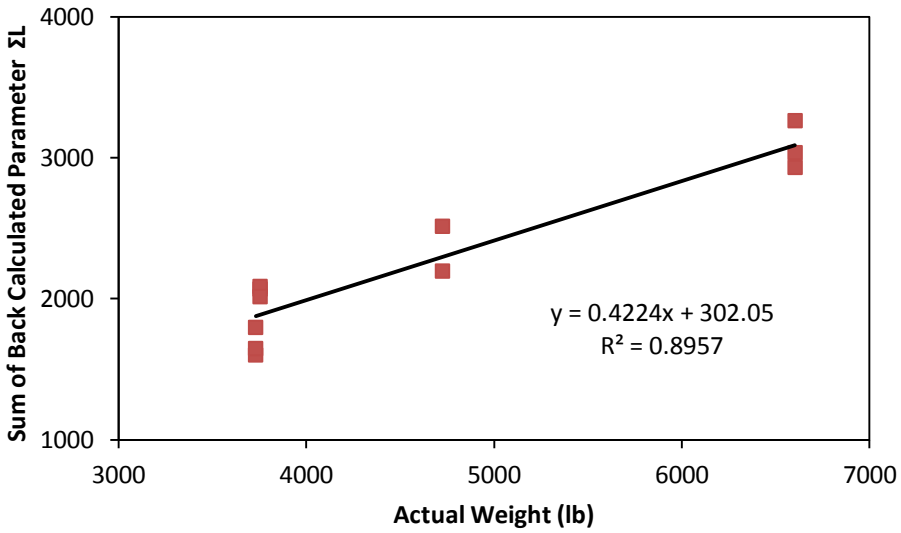

Figure 26: Back Calculated $\sum L$ and the Weight of Corresponding Vehicle

As shown in Figure 26, when temperature stays constant, $\sum L$ increases linearly with the actual weight of vehicles. Based on the linear relationship between $\sum L$ and vehicle weight, the back calculation of weight is simplified into Eq. (23) and (24).

$$Wheel\ Load = CF \cdot R \cdot L \quad \text{Eq.(23)}$$

$$Weight = \sum Wheel\ Load_i \quad \text{Eq.(24)}$$

where R is the ratio between the wheel load and parameter L in ABAQUS, and CF is the factor to correct the difference between theoretical calculation and actual application.

For example, when temperature is 18.1°C, R is calculated to be 7.607 from Table 5, and CF is 0.7886 from the regression of on-site calibration. Back calculated wheel load of Vehicle #1 are summarized in Table 7.

Table 7: Back Calculated Wheel Load of Testing Vehicle #1 (lb)

	Front Tires		Rear Tires		Total
	Left	Right	Left	Right	
Run #1	1,795.1	1,021.2	2,574.7	1,242.9	6,633.8
Run #2	1,795.5	1,358.0	2,141.3	1,198.2	6,493.0
Run #3	2,492.2	715.4	2,760.2	465.3	6,433.1

As seen in Table 7, the load distribution over the four tires of the moving vehicle changes with a big turbulence, this makes this dynamic problem even more complicated. However, the calculated total weight keeps around the actual weight 6520 lb (vehicles' weight plus one driver), which validates the Weigh-In-Motion function of this monitoring system again.

Summary

Viscoelastic pavement loading processes modeled in ABAQUS, and the simulated strain distribution match with measured data in experiment well in the trend (**Error! Reference source not found.**). The deviation is normal for a viscoelastic dynamic loading process on asphalt concrete. The ABAQUS viscoelastic model proved to be reliable for pavement response simulation under moving loads.

Bell Curved Model is used to simulate the spatial distribution of horizontal strain. The designed parameters in the model are assumed to be related with some parameters of passing load, including wheel load, width of tire, and passing offset distance. The parameter μ corresponds to offset of the maximum strain response for each tire. The distance between wheels can be calculated according to the offset of the tires on same axle. The parameter σ presents a second order polynomial relationship with the tire width. The parameter L, which is actually the area under Gaussian function, proved to be related to the wheel load.

Bell Curved Model is verified in ABAQUS with changing offset distance, contact area and applied load, and the parameters present expected relationships with passing load (**Error! Reference source not found.**). The back calculations method also showed good performance in

On-site testing with different vehicles. The verifications with both ABAQUS and on-site testing make the Bell Curved Model more convincing.

Traffic volume can be monitored by the sum of strain responses collected in the transverse plane (A5-A9 or B5-B9). Speed of each vehicle can be calculated based on the time interval between sensors, and distance between axles is based on the calculated speed and time interval between axles. The distance between axles can be obtained based on back calculated position of each wheel. The load of each wheel can be estimated based on the area under the strain distribution curve in transverse plane.

There is certain deviation between the calculated speed and speed gun reading, and error might be induced by speed gun reading, inaccurate sensor installation, and low frequency of data collecting, and so on. This distance refers to the outer edge to outer edge distance of wheels instead of center to center, probably because the highest pressure happens at the edge of the tires, and leads to the maximum responses in pavement.

An example of back calculation method is provided, and can be used to count traffic and collect the weight, speed and configuration of passing vehicles only with ten normal strain gauges in pavement. Gaussian function is used in the back calculation to model the horizontal strain distribution via offset distance, and the simulated parameter of Gaussian function is correlated to weight and configuration parameters of passing vehicles directly. The advantages of this system are summarized as following:

- The accuracy of back calculated traffic statistics is acceptable;
- The time cost for analysis is low, probably hundredths of a second for a normal laptop;
- Ignorable storage requirement compared to image processing method. Only several numbers can be stored for each passing vehicle after analysis (speed, configuration parameters, and classification categories);
- Can be integrated with other monitoring systems easily, for example, pavement health monitoring and Weigh-In-Motion systems.

Based on the advantages described above, this method can be recognized as very efficient and valuable for Intelligent Transportation System. In future, this method can be improved by

increasing number of sensors, enlarging sample sizes, and take more environmental factor into consideration.

CONCLUSIONS

Transportation related monitoring system is very important, and has been developed a lot in the last two decades. In this project, a wireless sensing network was designed and deployed. Based on the sensing network, mechanical responses were collected and used to monitor the health status of the experimental pavement section. At the same time, the data collected with the sensing network was also used to back calculate various loading related parameters of passing vehicles, which can be used as traffic information for intelligent transportation systems.

The developed wireless sensing network included four kinds of pavement sensors: strain gauges, load cells, thermocouple, and moisture sensor. One load cell and strain gauges in different directions are set as a group with the same transverse position, and were thought to collect different responses at the same point without any wandering. Five horizontal strain gauges are arranged longitudinally in the same transverse plane to recognize the exact passing position in transverse plane. Commercially off-the-shelf wireless nodes and base station were used as data loggers to transfer the collected responses to a laptop wirelessly for analysis.

In the pavement health status monitoring system, the strain, stress, temperature and moisture responses were collected and analyzed continuously in real-time monitoring. Finite Element Method based analysis software ABAQUS was used, and numerical simulation was performed based on visco-elastic material model. The simulated strain distribution was proved close to the collected signals on trend and magnitude under same temperature and similar loading condition. The ratio R_{ZX} between vertical stress σ_Z and horizontal strain ε_X was proved to be related to the pavement elastic modulus, and used to back calculate the elastic modulus of asphalt concrete layer. Pavement modulus back calculation can be conducted every half/one year to track the structural strength of pavements for health monitoring purpose. The pavement strain response for each passing vehicle can be collected and used for pavement fatigue cracking and rutting damage induced by the single pass. The damage of each passing vehicle can be cumulated for pavement service life prediction and life cycle management.

In the traffic information back calculation system, a bell-shaped model based on Gaussian function was used to describe the strain responses from the distributed strain gauges in each

wheel path. The parameters of Bell-Curve model were proved to be related with position, contact area and loading magnitude of the passing load in ABAQUS simulation. Then each passing wheel was modeled with Bell-Curve model and the simulated parameters were used to back calculate the wandering position, distance between wheels, width of tires, and axle loads. At the same time, the continuous strain signals from the distributed horizontal strain gauges can also be used to count the traffic volume and back calculate the speed of passing vehicles. All back calculations were proved to be effective in the experiments.

the developed wireless system, was titled integrated transportation monitoring system as the embedded sensors were used to concurrently monitor the pavement health status and collect traffic information , . This transportation monitoring system has the following advantages:

- Low cost. No large financial and manpower cost is necessary during the installation, data collection and maintenance of the system.
- Multi functionalities. Both pavement and traffic flow are being monitored by this system.
- High efficiency. The calculation process efficiently predicts the distress and the back calculation of pavement modulus and traffic information, and no large computer or data storage space is necessary.

In this study, two monitoring systems for traffic information and pavement health monitoring were designed and developed based on the same pavement sensing units. In the future, the calculation functions can be improved by taking temperature and additional loading conditions into consideration. Hence, this integrated monitoring system can be used as a comprehensive transportation information collection system, as is valuable for intelligent transportation systems and socialized infrastructure management.

APPENDIX

Appendix A: Specifications of Devices

A1 Specifications of V-Link 2.4 GHz Wireless Voltage Node

Input channels	Up to 8 input channels: 4 full differential (350 Ω resistance or higher); 3 single ended input (0~3 volts maximum); 1 internal temperature sensor
Temperature sensor	-40°C to 70°C range, typical accuracy ±2°C (at 25°C)
Anti-aliasing filter bandwidth	-3 dB cutoff at 250 Hz
Measurement Accuracy	±0.1% full scale typical
Resolution	1 bit: 0.024%
DC bridge excitation	+3 volts DC at 50 mA maximum
Programmable gain	Software programmable for differential input channels from 210 to 4844
Programmable offset	Software programmable
Analog to digital (A/D) converter	Successive approximation type, 12 bit resolution
Data storage capacity	2 megabytes (approximately 1,000,000 data points)
Data logging mode	Log up to 1,000,000 data points (from 100 to 65,500 samples or continuous) at 32 Hz to 2048 Hz
Sensor event driven trigger	Commence datalogging when threshold exceeded
Real-time steaming mode	Transmit real time data from node to PC – rate depends on number of active channels: 1 channel – 4 KHz; 2 channel – 2 KHz; 3 channel – 1.33 KHz; 4 channel – 1 KHz; 5 channel – 800 Hz; 6 channel – 666 Hz; 7 channel – 570 Hz; 8 channel – 500 Hz;
Low duty-cycle mode	Supports multiple nodes on single RF channel from 1 sample per hour to 250 Hz
Synchronization between nodes	Datalogging ±4 µsec ±50 ppm, LDC mode time stamped at PC
Sample rate stability	±25 ppm for sample rates > 1 Hz, ±10% for sample rates ≤ 1 Hz
Wireless shunt calibration	Channels 1 to 4, internal shunt calibration resistor 499 KΩ
Radio frequency (RF) transceiver carrier	2.4 GHz direct sequence spread spectrum, license free worldwide (2.405 to 2.480 GHz) – 16 channels, radiated power 0 dBm (1 mW)
RF data packet standard	IEEE 802.15.4, open communication architecture
RF data downloading	8 minutes to download full memory
Range for bi-directional RF link	70 m line-of-sight, up to 300 m with optional high gain antenna
Internal Li-Ion battery	3.7 volt lithium ion rechargeable battery, 740 mAh capacity; customer may supply external power from 3.2 to 9 volts
Power consumption	V-Link node only: real-time straming – 25 mA; datalogging – 25 mA; sleeping – 0.1 Ma. External sensors: 350 Ω strain gauge – 8 mA; 1000 Ω strain gauge – 3 mA.
Operating temperature	-20°C to +60°C with standard internal battery and enclosure, extended temperature range optional with custom battery and enclosure, -40°C to +85°C for electronics only
Maximum acceleration limit	500 g standard
Dimensions	88 mm × 72 mm × 26 mm (enclosure without antenna). 76 mm × 65 mm × 12 mm (circuit board assembly only).
Weight	97 g (with enclosure), 15 g (circuit board assembly only).
Enclosure material	ABS plastic
Software	Node Commander Windows XP/Vista compatible
Compatible base stations	USB, RS-232, Analog, WSDA

A2 Specifications of CTL Asphalt Strain Gage

General Specifications	
Bridge Completion	Full bridge
Gage Resistance	350 Ohm
Excitation	Up to 10 Volts
Output	≈2mV/V @ 1500 μstrain
Grid Area	0.133 cm^2
Gage Area	1.22 cm^2
Fatigue Life	<105 repetitions @ +/- 2000 μstrain
Modulus	340,000 psi
Cell Material	Black 6/6 nylon
Coating	Two-part polysulfide liquid polymer encapsulated in silicone with butyl rubber outer core
Quality Assurance	
Water Submersion	1 ft for 24 hours at 24 °C (75 °F)
Temperature	-34 °C (-30 °F) TO 204 °C (400 °F)
Lead Wire	30 ft of 22 AWG braided shield four wire

A3 Specifications of Load Cell KDE-PA

Capacity	2 MPa
Rated output	0.5 mV/V (1000 μstrain)
Non-linearity	2%RO
Temperature range	-20 ~ +60 °C
Input/Output resistance	350 Ohm
Recommended exciting voltage	Less than 3V
Allowable exciting voltage	10 V
Weight	160 g

A4 Specifications of Thermo Couple TMTSS-125-6

Length	6 inch
Sheath diameters	0.125 inch
Junction Type	Grounded
Wires	40 inch Teflon-Coated lead wires
Upper Temperature	°C (500°F)

A5 Specifications of Moisture Sensor VH400

Power consumption	<7 mA
Supply Voltage	3.3V to 20 VDC
Output Impedance	100 K Ohm
Operational temperature	-40 °C to 85 °C
Frequency of operation	80 MHz
Accuracy	2%
Output	0~3V related moisture content
Sensitive to volume	No
Sensitive to salt	No
Shell Color	Red

Appendix B: Asphalt Concrete Job-Mix Formula

TL-127 MC (11-06)

VIRGINIA DEPARTMENT OF TRANSPORTATION

MATERIALS DIVISION

STATEMENT OF ASPHALT CONCRETE OR CENTRAL-MIX AGGREGATE JOB-MIX FORMULA

Submit to the District Administrator, Virginia department of Transportation. Approval must be received by ther contractor from the Materials Division before work is begun. This job-mix design is approved for all projects of the Department for the type of mix and the calendar year shown below.

Contractor Design Mix No.	2007 201116			Design Lab No.	S-1
Date	7/13/2011	Job Mix ID No.		Calendar Yr. 2011	TSR Test No. 0%
Type Mix / Size Aggregate	SM-9.5D HR				
Producer Name & Plant Location	Adams Construction Co. -	Rockydale II		Phone	(540) 774-4419

Materials				Kind	Source
Approval Phase	A	B *	C		
Aggregate	49.0%	49.0%		#8 AMPHIBOLE	ROCKYDALE QUARRY - GLADE HILL, VA
Aggregate					
Aggregate					
Screening	8.0%	8.0%		#10 LIMESTONE	ROCKYDALE QUARRY - ROANOKE, VA
Sand	18.0%	18.0%		NATURAL	CASTLE SAND CO. - NEW CASTLE, VA
RAP	25.0%	25.0%		PROCESSED	ADAMS CONSTRUCTION CO. - ROANOKE, VA
Lime					
Asphalt Cement	5.5%	5.5%		PG 64-22	ASSOCIATED ASPHALT - ROANOKE, VA
Additives	0.5%	0.5%		ADHERE HP+	ARR-MAZ PRODUCTS - WINTER HAVEN, FL

Job Mix Sieves	Total % Passing		Tolerance % + or -	Acceptance Range Average of 8 Tests		End of Year Average	Design/Spec. Range
	Lab JMF	Producton JMF					
Approval Phase	A	B *		A	B	C	
1/2"	100.0	100.0	0	100.0	100		100
3/8"	94.0	97.0	2.8	91.2 - 96.8	94.2 - 99.8		90 - 100
#4	55.0	58.0	2.8	52.2 - 57.8	55.2 - 60.8		80 MAX
#8	40.0	40.0	2.8	37.2 - 42.8	37.2 - 42.8		38 - 67
#200	5.7	5.7	0.7	5.0 - 6.4	5.0 - 6.4		2 - 10
Asphalt (%)	5.5	5.5	0.21	5.29 - 5.71	5.29 - 5.71		

Lay Down Temperatures	270 - 350	°F (°C)	Muffle Furnace Correction Factor:	0.04
			Field Correction Factor (Gse - Gsb):	0.019
Lab Compaction Temperatures	295 - 300	°F (°C)	Pill Weight:	5150
			SMA Mixes	
Producer Technician's Certification Number	M. WALLACE		VCA drc:	
			Gca:	

MATERIALS DIVISION USE ONLY 0

Calculated Mix PG Grade: 71.87

Remarks	VMA = 16.6		VFA = 78.7		F/A = 1.08		PERM <80		Gse = 2.898		Pbe = 5.28
Nominal Max. Size Aggregate			Application Rates:		Min.		lb/yd^2		Max.		lb/yd^2
Mix Properties at the Job-Mix Asphalt Content:		Compacted Unit Weight		158.7	lb.ft^3		VTM:	3.5	Gmm:		2.635

Checked By:	Jeff Henderson				*Potential VFA & F/A problems*		
Approved tenetatively subject to the production of material meeting all other applicable requirements of the specification.							
* Note: Part B "Production JMF" and corresponding Materials percentages will be filled out by the DME upon receipt of the additional requirements of the HMA producer within the first lot under Section 502.01(b).							
Copies:	State Materials Engineer	Approvals	☑	Part A:	D. Clyde Landreth	Date:	7/14/2011
	District Materials Engineer		☑	Part B:	D. Clyde Landreth	Date:	10/26/2011
	Project Inspector		☐	Part C:		Date:	
	Sub-Contractor and/or Producer						

REFERENCES

1. Corley-Lay, J., et al., *Comparison of Flexible Pavement Distresses Monitored by North Carolina Department of Transportation and Long-Term Pavement Performance Program.* Transportation Research Record: Journal of the Transportation Research Board, 2010. **2153**: p. 91-96.

2. Cheng, H., et al., *Novel Approach to Pavement Cracking Detection Based on Fuzzy Set Theory.* Journal of Computing in Civil Engineering, 1999. **13**(4): p. 270-280.

3. Amarasiri, S., et al., *Optical Texture-Based Tools for Monitoring Pavement Surface Wear and Cracks Using Digital Images.* Transportation Research Record: Journal of the Transportation Research Board, 2010(2153): p. 130-140.

4. Mohajeri, M.H. and P.J. Manning, *ARIA: an operating system of pavement distress diagnosis by image processing.* Transportation Research Record: Journal of the Transportation Research Board, 1991(1311): p. 120-130.

5. Koutsopoulos, H. and A. Downey, *Primitive Based Classification of Pavement Cracking Images.* Journal of Transportation Engineering, 1993. **119**(3): p. 402-418.

6. Hass, C. and H. C., *Computer-based model of pavement surface.* Transportation Research Record: Journal of the Transportation Research Board, 1990(1260): p. 91-98.

7. Walker, R.S. and R.L. Harris, *Noncontact pavement crack detection system.* Transportation Research Record: Journal of the Transportation Research Board, 1991(1311): p. 149-157.

8. Chou, J., W.A. O'Neill, and H. Cheng, *Pavement distress evaluation using Fuzzy logic and moment invariants.* Transportation Research Record: Journal of the Transportation Research Board, 1995(1505): p. 39-46.

9. *NCHRP 1-26, Calibrated Mechanistic Structural Analysis Procedures for Pavement*, in *National Cooperative Highway Research Program Project 1-26,*1990, Transportation Research Board: Washington D.C. p. 90.

10. Ahlvin, R.G., et al., *Multiple-Wheel Heavy Gear Load Pavement Tests*, in *Technical Report No AFWL-TR-70-113*1971, ARMY ENGINEER WATERWAYS EXPERIMENT STATION VICKSBURG MS. p. 95.

11. Mills, J.P., I. Newton, and G.C. Peirson, *Pavement Deformation Monitoring in a Rolling Load Facility.* The Photogrammetric Record, 2001. **17**(97): p. 7-24.

12. McQueen, R.D., W. Marsey, and J.M. Arze, *Analysis of Nondestructive Test Data on Flexible Pavements Acquired at the National Airport Pavement Test Facility*, in

Advancing Airfield Pavements, American Society of Civil Engineers: Reston, VA. p. 267-278.

13. Gopalakrishnan, K., *Condition monitoring of bituminous pavements subjected to repeated dynamic aircraft loading.* The Baltic journal of road and bridge engineering, 2006. **1**(3): p. 135-142.

14. Haider, S.W., et al., *Impact of Pavement Monitoring Frequency on Pavement Management System Decisions.* Transportation Research Record: Journal of the Transportation Research Board, 2011. **2225**(-1): p. 43-55.

15. McGhee, K.H., *NCHRP Synthesis of Highway Practice 334: Automated Pavement Distress Collection Techniques*, 2004, Transportation Research Board of the National Academies: Washington D.C.

16. Potter, J.F., H.C. Mayhew, and A.P. Mayo, *Instrumentation of the Full Scale Experiment on A1 Trunk Road at Conington, Huntingdonshire*, in *Report LR296, Road Research Lab /UK/*1969. p. 41.

17. Sebaaly, P.E., et al., *Instrumentation for Flexible Pavements - Field Performance of Selected Sensors*, 1991, Federal Highway Administration: Washington D.C.

18. Sebaaly, P.E., N. Tabatabaee, and B. Kulakowski, *EVALUATION OF THE HALL-EFFECT SENSOR FOR PAVEMENT INSTRUMENTATION.* Journal of Testing and Evaluation, 1995. **23**(3): p. 189-195.

19. Goncalves, F.P., J.A.P. Ceratti, and A.V.D. Bica, *The use of embedded stress cells for monitoring pavement performance.* Geotechnical testing journal, 2003. **26**(4): p. 363-372.

20. Huff, R., C. Berthelot, and B. Daku, *Continuous primary dynamic pavement response system using piezoelectric axle sensors.* Canadian journal of civil engineering, 2005. **32**(1): p. 260-269.

21. Xue, W.J. and E. Weaver, *Pavement Shear Strain Response to Dual and Wide-Base Tires.* Transportation Research Record, 2011(2225): p. 155-164.

22. Lajnef, N., et al., *Toward an Integrated Smart Sensing System and Data Interpretation Techniques for Pavement Fatigue Monitoring.* Computer-Aided Civil and Infrastructure Engineering, 2011. **26**(7): p. 513-523.

23. Malla, R., A. Sen, and N. Garrick, *A Special Fiber Optic Sensor for Measuring Wheel Loads of Vehicles on Highways.* Sensors, 2008. **8**(4): p. 2551-2568.

24. Li, H.N., D.S. Li, and G. Song, *Recent applications of fiber optic sensors to health monitoring in civil engineering.* Engineering Structures, 2004. **26**: p. 1647-1657.

25. Navarrete, M.C. and E. Bernabeu, *Fibre-optic weigh-in-motion sensor.* Sensors and Actuators A: Physical, 1994. **41**(1–3): p. 110-113.

26. Signore, J.M. and J.R. Roesler, *Using Fiber-Optic Sensing Techniques to Monitor Behavior of Transportation Materials.* Transportation Research Record: Journal of the Transportation Research Board, 1995. **1478**: p. 37-43.

27. Wang, J.N. and J.L. Tang, *Using fiber Bragg grating sensors to monitor pavement structures.* Transportation Research Record: Journal of the Transportation Research Board, 2005. **1913**: p. 165-176.

28. Zhou, Z., et al., *Optical fiber Bragg grating sensor assembly for 3D strain monitoring and its case study in highway pavement.* Mechanical Systems and Signal Processing, 2012. **28**: p. 36-49.

29. Timm, D.H., A.L. Priest, and T.V. McEwen, *Design and instrumentation of the structural pavement experiment at the NCAT test track*, 2004, National Center for Asphalt Technology, Auburn University.

30. Rollings, R.S. and D.W. Pittman, *Field Instrumentation and Performance Monitoring of Rigid Pavements.* Journal of Transportation Engineering, 1992. **118**(3): p. 361-370.

31. Timm, D.H. and A.L. Priest, *Dynamic pavement response data collection and processing at the NCAT test track*, 2004, National Center for Asphalt Technology, Auburn University. .

32. Lukanen, E.O., *Load testing of instrumented pavement sections*, 2005, Minnesota Department of Transportation, Research Services Section.

33. Al-Qadi, I.L., et al., *The Virginia Smart Road: the impact of pavement instrumentation on understanding pavement performance.* The Journal of APPT, 2004. **73**: p. 427-465.

34. Loulizi, A., I. Al-Qadi, and M. Elseifi, *Difference between In Situ Flexible Pavement Measured and Calculated Stresses and Strains.* Journal of Transportation Engineering, 2006. **132**(7): p. 574-579.

35. Hipley, P. *Caltrans' Current State-of-Practice*. in *Instrumental Diagnostics of Seismic Response of Bridges and Dams*. 2001. University of California, Berkeley: Pacific Earthquake Engineering Research Center.

36. Lynch, J.P., et al., *Performance monitoring of the Geumdang Bridge using a dense network of high-resolution wireless sensors.* Smart Materials and Structures, 2006. **15**(6): p. 1561-1575.

37. Ko, J. and Y. Ni, *Structural health monitoring and intelligent vibration control of cable-supported bridges: Research and application.* KSCE Journal of Civil Engineering, 2003. **7**(6): p. 701-716.

38. Barrish, J.R.A., *Instrumented monitoring of the Commodore Barry Bridge.* Proceedings of SPIE, the international society for optical engineering, 2000. **3995**(1): p. 112-126.

39. Kim, J. and J.P. Lynch, *Experimental analysis of vehicle–bridge interaction using a wireless monitoring system and a two-stage system identification technique.* Mechanical Systems and Signal Processing, 2012. **28**(0): p. 3-19.

40. Norman, O. and R. Hopkins. *Weighing Vehicles in Motion*. in *31st Annual Meeting of Highway Research Board*. 1952. Washington D.C.: Highway Research Board.

41. George, Y. and C. Antoniou, *Integration of Weigh-in-Motion Technologies in Road Infrastructure Management.* ITE Journal, 2005. **75**(1): p. 39-43.

42. Lu, Q., et al., *Truck traffic analysis using Weigh-in-Motion (WIM) data in California*, 2002, University of California, Berkeley, Institute of Transportation Studies, Pavement Research Center.

43. Cheng, L., H. Zhang, and Q. Li, *Design of a capacitive flexible weighing sensor for vehicle WIM system.* Sensors, 2007. **7**: p. 1530-1544.

44. *Standard Specification for Highway Weigh-in-Motion (WIM) Systems with User Requirements and Test Methods*, in *ASTM Standard E1318-09*1994, American Society for Testing and Materials.

45. Stamatinos, G. and J. Wyatt, *EVALUATION OF IRD-WIM-5000 - A CANADIAN WEIGH-IN-MOTION SYSTEM*. Canadian journal of civil engineering, 1990. **17**(4): p. 514-520.

46. Yuan, S., et al., *Optic fiber-based dynamic pressure sensor for WIM system.* Sensors and Actuators A: Physical, 2005. **120**(1): p. 53-58.

47. Teral, S.R., et al., *Fiber optic weigh-in-motion sensor: correlation between modeling and practical characterization.* Proceedings of SPIE, the international society for optical engineering, 1996. **2718**(1): p. 417-426.

48. Muhs, J.D., et al., *Results of a portable fiber optic weigh-in-motion system.* Proceedings of SPIE - International Society for Optical Engineering 1991. **1584**: p. 374-386.

49. Kenneth W. Tobin, J. and J.D. Muhs, *Algorithm for a novel fiber optic weigh-in-motion sensor system.* Proceedings of SPIE - International Society for Optical Engineering 1991. **1589**: p. 102-109.

50. Cheng, L., H. Zhang, and Q. Li, *Design of a Capacitive Flexible Weighing Sensor for Vehicle WIM System.* Sensors, 2007. **7**(8): p. 1530-1544.

51. Zhang, W., C. Suo, and Q. Wang, *A Novel Sensor System for Measuring Wheel Loads of Vehicles on Highways.* Sensors, 2008. **8**: p. 7671-7689.

52. Nash, D.D., *Alice: Automatic Length Indication and Classification Equipment. An Equipment for Automatically Classifying Vehicles and Measuring Their Speed.* Traffic Engineering and Control, 1976. **17**(12): p. 496-501.

53. Benekohal, R. and M. Girianna, *Technologies for Truck Classification and Methodologies for Estimating Truck Vehicle Miles Traveled.* Transportation Research Record: Journal of the Transportation Research Board, 2003. **1855**(-1): p. 1-13.

54. Gajda, J., et al. *A vehicle classification based on inductive loop detectors*. in *Instrumentation and Measurement Technology Conference, IMTC 2001. Proceedings of the 18th IEEE*. 2001.

55. Coifman, B. and S. Kim, *Speed estimation and length based vehicle classification from freeway single-loop detectors.* Transportation Research Part C: Emerging Technologies, 2009. **17**(4): p. 349-364.

56. Coifman, B., *Improved velocity estimation using single loop detectors.* Transportation Research Part A: Policy and Practice, 2001. **35**(10): p. 863-880.

57. Kwon, J., P. Varaiya, and A. Skabardonis, *Estimation of Truck Traffic Volume from Single Loop Detectors with Lane-to-Lane Speed Correlation.* Transportation Research Record: Journal of the Transportation Research Board, 2003. **1856**(-1): p. 106-117.

58. Yinhai, W. and N.L. Nihan, *Dynamic Estimation of Freeway Large-Truck Volumes Based on Single-Loop Measurements.* Journal of Intelligent Transportation Systems, 2004. **8**(3): p. 133-141.

59. Udd, E., et al., *Fiber grating systems for traffic monitoring.* Proceedings of SPIE - International Society for Optical Engineering 2001. **4337**: p. 510-516.

60. Kunzler, M., et al., *Fiber grating traffic monitoring systems.* Proceedings of SPIE - International Society for Optical Engineering 2002. **4696**: p. 238-243.

61. Kunzler, M., et al., *Traffic monitoring using fiber optic grating sensors on the I-84 freeway and future uses in WIM.* Proceedings of SPIE - International Society for Optical Engineering 2003. **5278**: p. 122-127.

62. Kunzler, M., et al., *Second-generation fiber grating traffic monitoring systems on the I-84 freeway.* Proceedings of SPIE - International Society for Optical Engineering 2003. **5054**: p. 230-239.

63. Zhang, W., Q. Wang, and C. Suo, *A Novel Vehicle Classification Using Embedded Strain Gauge Sensors.* Sensors, 2008. **8**(11): p. 6952-6971.

64. *Traffic Monitoring Handbook*, 2007, Florida Department of Transportation.

65. Cosentino, P.J., W. von Eckroth, and B.G. Grossman, *Analysis of fiber optic traffic sensors in flexible pavements.* Journal of Transportation Engineering-Asce, 2003. **129**(5): p. 549-557.

66. Cosentino, P.J. and B.G. Grossman, *Development and Implementation of a Fiber Optic Vehicle Detection and Counter System: Final Report*, in *FDOT Final Report*1996, Florida Institute of Technology, Melbourne, Florida.

67. Cosentino, P.J. and B.G. Grossman, *Development of Fiber Optic Dynamic Weight-in-Motion System*, in *FDOT Final Report*1997, Florida Institute of Technology, Melbourne, Florida.

68. Cosentino, P.J. and B.G. Grossman, *Optimization and Implementation of Fiber Optic Sensors for Traffic Classification and Weigh-in-Motion Systems, Phase 3*, in *FDOT Final Report*2000, Florida Institute of Technology, Melbourne, Florida.

69. Morgan, G.C.J.P., L. D.; Arraigada, M.; Partl, M. N.; Muff, R. , *In situ Monitoring of Pavement Stresses on the A1 in Switzerland.* Journal of Testing and Evaluation 2008. **36**(4): p. 1-9.

70. Wong, K.-y., C.K. Lau, and A.R. Flint, *Planning and implementation of the structural health monitoring system for cable-supported bridges in Hong Kong.* Proceedings of SPIE - International Society for Optical Engineering 2000. **3995**: p. 266-275.

71. Straser, E.G. and A.S. Kiremidjian, *A modular, wireless damage monitoring system for structures*, in *Technical Report*1998, John A. Blume Earthquake Engineering Center: Stanford, CA.

72. Lynch, J.P., et al., *Design and performance validation of a wireless sensing unit for structural monitoring applications.* Structural Engineering and Mechanics, 2004. **17**: p. 393-408.

73. Goel, A. and A. Das, *Nondestructive testing of asphalt pavements for structural condition evaluation: a state of the art.* Nondestructive Testing and Evaluation, 2008. **23**(2): p. 121-140.

74. Huang, Y.H., *Pavement analysis and design*2004, Upper Saddle River.

75. Huang, S. and A.W. Sadek, *A novel forecasting approach inspired by human memory: The example of short-term traffic volume forecasting.* Transportation Research Part C: Emerging Technologies, 2009. **17**(5): p. 510-525.

76. Abdulhai, B., H. Porwal, and W. Recker, *Short-term traffic flow prediction using neuro-genetic algorithms.* Its Journal, 2002. **7**(1): p. 3-41.

77. Lingras, P., et al., *Traffic volume time-series analysis according to the type of road use.* Computer-Aided Civil and Infrastructure Engineering, 2000. **15**(5): p. 365-373.

78. Jianming, H., et al., *Traffic congestion identification based on image processing.* Intelligent Transport Systems, IET, 2012. **6**(2): p. 153-160.

79. de-la-Rocha, E. and R. Palacios, *Speed estimation of vehicles approaching an intersection: a digital image processing method.* Imaging Science Journal, 2011. **59**(5): p. 293-302.

80. Haghani, A., et al., *Data Collection of Freeway Travel Time Ground Truth with Bluetooth Sensors.* Transportation Research Record: Journal of the Transportation Research Board, 2010. **2160**(-1): p. 60-68.